Forschungszentrum Karlsruhe

Technik und Umwelt

Wissenschaftliche Berichte

FZKA 6334

Modifications of the Code SAS4A for Simulation of ADS Designs

R. Dagan, C. H. M. Broeders , D. Struwe

Institut für Reaktorsicherheit
Institut für Kern und Energietechnik

Projekt Nukleare Sicherheitsforschung

Forschungszentrum Karlsruhe GmbH, Karlsruhe
2000

Als Manuskript gedruckt

Forschungszentrum Karlsruhe GmbH
Postfach 3640, 76021 Karlsruhe

Mitglied der Hermann von Helmholtz-Gemeinschaft
Deutscher Forschungszentren (HGF)

ISSN 0947-8620

Abstract

The current ADS (Accelerator Driven System) design is based on a fast core. Therefore it is quite natural to adapt the SAS4A code to an ADS simulation for transient analyses. The current study shows that the point kinetic model in SAS4A code enables the activation of an external source with relative few modifications. In addition, localized reactivity feedback coefficients and the power distribution in an ADS must be known for a SAS4A transient core simulation. The use of perturbation theory for ADS, successfully used in homogeneous problems, is still not resolved conclusively since some parameters are undefined, in particular the adjoint weighting function and the adjoint definition of the external source. The use of perturbation theory for the calculation of localized reactivity coefficients for ADS seems therefore not applicable. These reactivity coefficients can also be determined by means of successive criticality calculations. This can be done by determining differences of multiplicity factor depending on changes in local core materials properties against the original state. The enhanced computational time requirements are acceptable.

The codes package KAPROS was initially used in the current study to investigate the applicability of perturbation theory for ADS, and to demonstrate the differences between source free systems (using D3E/D3D codes) and ADS. In particular the R-Z option of the DIXY code which allows for correct multiplicity factor calculation, was used for ADS simulation.

Subsequently, the CITATION code was used to calculate the reactivity state for various core conditions. This code allows for the three dimensions hexagonal representation of any ADS configuration. The results of these calculations are then used to calculate all the relevant local reactivity perturbations. The collapsed multi-group cross-section sets, which serve as input to the CITATION code, were determined with the KAPROS code system. The three sources ADS configuration, which was selected as reference case in this study, can be modified to any desired configuration dependent on the particular requirements, such as transmutations optimization or some other relevant criteria.

Erweiterungen des Programms SAS4A zur Simulation von ADS Entwürfen

Zusammenfassung

Die hier untersuchte ADS-Referenzauslegung basiert auf einem schnellen Kern. Es ist deshalb sinnvoll, das SAS4A Codesystem zur Bererchnung von Störfalltransienten für ADS - Simulationen zu ertüchtigen. Die vorliegende Untersuchung zeigt, dass das punktkinetische Modell im SAS4A-Code die Aktivierung einer externen Quelle zulässt. Zur Durchführung von SAS4A ADS Transientenanalysen müssen jedoch Leistungsverteilung und lokale Reaktivitätskoeffizienten als Eingabe vorliegen. Die Anwendbarkeit von Störungstheorie bei ADS ist wegen der unbekannten Definition der adjungierten Wichtungsfunktion als auch dem adjungierten externen Quellterm noch nicht geklärt. Die Anwendung von Störungstheorie für ADS Systeme erscheint deshalb fraglich. Reaktivitätskoeffizienten können jedoch ebenfalls durch sukzessive Reaktivitätsrechnungen bestimmt werden. Dies kann erreicht werden, indem die Reaktivitätsveränderungen durch die Änderungen der örtlichen Kern-Materialeigenschaften relativ zum Referenzzustand bestimmt werden. Der hierdurch entstehende höhere Rechenbedarf ist akzeptabel.

In der vorliegenden Untersuchung wurde zunächst das Rechenprogrammsystem KAPROS eingesetzt, um die Unterschiede zwischen quelle-freien Systemen (durchgeführt mit D3E/D3D Rechenprogrammen) und ADS zu klären. Dabei wurde die R-Z Option des DIXY2-Programms verwendet, dessen numerisches Verfahren die Ermittlung des Multiplikationsfaktors einer ADS-Anordnung ermöglicht.

Daraufhin wurde das Rechenprogramm CITATION eingesetzt, welches eine dreidimensionale, hexagonale Repräsentation des ADS ermöglicht. Mit CITATION kann eine genaue Bestimmung des Einflusses von lokalen Veränderungen auf den Reaktivitätszustand der Anordnung bestimmt werden. Der Code wurde zur Optimierung einer Kernkonfiguration für ein ADS auf der Basis eines Kerns mit frischem Brennstoff eingesetzt. Die Dreiquellenkonfiguration, die dieser Untersuchung als Referenzauslegung zugrunde gelegt wurde, kann den Auslegungkriterien, z.B. Optimierung zur Transmutation, entsprechend verändert werden.

Contents

List of Tables

List of Figures

Nomenclature[1]

Greek Symbols

α	Void fraction

Subscripts

$+$	Adjoint
eff	effective

Abbreviations

ADS	Accelerator Driven System
HM	Heavy Metal
LLFP	Long Live Fission Products
SA	Subassembly
SAS4A	LMFBR Accident Analysis Code System

[1]Variables and Symbols not included here are explained there where they appear first.

1 Introduction

In the last decade considerable effort was devoted to finding innovative solutions for radioactive waste disposal, in particular by transmutation of the so called "LLFP-Long Live Fission Products" of the burned fuel. At the same time the demand for cores with advanced inherent safety features, was increased. One of the suggested solutions to enhance the safety of nuclear energy production within a system, which is also capable of incinerating radioactive actinides efficiently, was the Accelerator Driven System (ADS). This type of reactor is unique in the nuclear field as it is a combination of a subcritical core and an accelerator which injects protons into the system. The protons bombard a spallation target located in the core, and thus thirty to fifty free neutrons are released . It is claimed [4] that such a device is very safe due to the lower probability of the core to become super-critical. The proposed device should supply power and at the same time incinerate the radioactive actinides which are inserted in the fuel matrix or in the blanket. Several considerations were taken into account for choosing the appropriate type of reactor to be used within an ADS. First, the amount of actinides the core can incinerate, compared with the fission products, produced during normal operation. Second aspect concerns the inherent safety features during unexpected transient incidents. One of the favorable core types to comply with those requirements, is believed to be the fast reactor cooled by lead (instead of the usual sodium cooled design) to avoid high positive void reactivity feedbacks. Additionally, the fast spectrum systems have the essential advantage of producing a surplus of neutrons. It is shown [17] that the transmutation rate (transmutations per fission) for a fast spectrum is higher than for other energy spectrum types.

The code SAS4A[1] is considered to be one of the best thermodynamics, transient analysis code for fast reactors. As the ADS design is based on a fast core design, it is quite natural to try to adapt the SAS4A code to an ADS simulation. The current study is dedicated to this task. The complex algorithm required to implement the ADS feature in SAS4A is discussed first. The technique for solving the neutronic part of the code in the presence of an additional external source is described. It is emphasized, that the current version of the code do not handle dynamical spatial transients, which are even more important when an external source is activated within the core.

The second part of the study refers to the reactivity feedback analysis of ADS, which is more complicated as it cannot use the well known eigenvalue solution technique (for critical assemblies) as it is not applicable for inhomogeneous problems. Thereafter, the implicit usage of first order perturbation theory in SAS4A code is questionable and should be revised.

After careful examination of the current version and the unique features of an ADS, the essential and available modifications within SAS4A for ADS simulation, are proposed in this study.

2 External Source Activation in SAS4A

2.1 Neutronic model of SAS4A

The calculations of the transient phenomena in SAS4A [1] following thermodynamic disturbances are based on a point kinetics model, which handles the equations for up to six groups of delayed neutrons precursors. The point kinetics model is valid, if the spatial flux shape changes significantly slower than does the flux amplitude. In a quasi-static approach [12] indeed, very few shape function calculations are needed (to achieve a reasonable accuracy) in comparison with the number of amplitude function recalculations. In SAS4A the above argument is stretched to its extreme extent by neglecting totally the spatial flux shape recalculation. There follows an underlying supposition implicitly implemented in the code namely, fluctuations in the reactor local parameters (geometry, dimensions, temperature and density) have minor effect on the overall spatial flux distribution. This assumption considerably reduces the complexity and computational expenses of the overall neutronics calculations (as is needed for example in the quasistatic treatment), with some loss of accuracy, (if fast reactors are considered). In particular, the simplicity of the calculations refers to the possibility of using first order perturbation theory, which is in full agreement with constant flux distribution assumption of the SAS4A code.

First order perturbation theory is based on using unperturbed flux [15] as it is sufficient for first order accuracy. Consequently, one can calculate reactivity feedbacks (regarding material temperature, density, relocations and void changes) separately for each of all the pin segments, using the same initial flux. Furthermore, all the local reactivity feedback contributions can be summed up linearly. This results in, a single overall reactivity feedback which is reinserted in the point kinetics model. In this procedure, the usage of unperturbed flux meets the requirement of constant flux distribution which is the fundamental basis of the channel structure (and its time independent power distribution) as well as the point kinetics model in SAS4A.

The goal of the current research is to enable the code SAS4A to deal with an ADS -Accelerator Driven System- which is a combination of an external source and a fast reactor. For such a subcritical system, the assumption of constant flux shape is doubtful in the case of transient simulations. In the next chapter, the spatial flux shape sensitivity to local disturbances (when ADS is considered) is examined. It is worthwhile to mention that in principle SAS4A could still simulates transient states, even if ADS is considered, as it has restart options in which the original imposed flux distribution can be modified. Such modifications are essential as is shown in the next chapter. Here however, the focus will remain only on the implementation of the external source in SAS4A regardless of possible distortions in the spatial flux distribution. (bearing in mind, the insertion of modified flux shapes is possible if needed).

The solution technique of the point kinetics equation is based on [2] and was modified to its current version by [3]. The point kinetics algorithm in [3] allows for several physical phenomena, such as fuel motion , subcritical reactor and an external source, which are denoted by ζ_i , k_0 , Q respectively in the following point kinetics equations:

$$\frac{dN}{dt} = \left(\frac{\rho - \beta}{\Lambda} + \frac{k_0 - 1}{\Lambda k_0}\right) N \ + \sum_{i=1}^{m} \lambda_i C_i + \sum_{i=1}^{m} \lambda_i \zeta_i + Q \qquad (1)$$

and:

$$\frac{dC_i}{dt} = \frac{\beta_i'}{\Lambda} N - \lambda C_i \qquad (2)$$

where
$N-$ amplitude function of the reactor power.
$\rho-$ reactivity.
$\beta-$ effective delayed neutron fraction.
$\beta_i'-$ effective delayed neutron fraction for the i^{th} family as calculated on a moving mesh.
$\Lambda-$ mean generation time.
$Q-$ external source
λ_i- decay constant of the i^{th} precursor family.
C_i- concentration of the i^{th} precursor family.
$m-$ number of neutrons precursor group (usually 6).
ζ_i- correction to concentration of i^{th} precursor family due to fuel motion.
k_0- eigenvalue of source-free equation (unity, unless the reactor is initially

subcritical)

The solution is based on integrating the six delayed neutron precursors equations over a time interval $t_{j-1} \leq t \leq t_j$. The expressions obtained for the delayed neutron precursors (C_i) are substituted into Eq. (1):

$$\frac{dN}{dt} = \left(\frac{\rho-\beta}{\Lambda} + \frac{k_0-1}{\Lambda k_0}\right) N +$$

$$\sum_{i=1}^{m} \lambda_i \left[C_i(t_{j-1}) \exp\left\{ -\int_{t_{j-1}}^{t} \lambda_i d\tau \right\} + \int_{t_{j-1}}^{t} \exp\left\{ -\int_{t_{j-1}}^{t} \lambda_i d\tau \right\} \frac{\beta'(t')}{\Lambda(t')} N(t') dt' + \zeta_i(t) \right]$$
$$+Q \qquad (3)$$

Thus instead of handling the "usual" 7 differential equations one is left with one differential equation which includes an integral part.

Next the power $N(t)$ is expressed by the following trial solution

$$N_K(t) = \sum_{k=0}^{K} A_k (t - t_{j-1})^k \qquad (4)$$

and also:

$$\frac{dN_K}{dt} = \sum_{k=0}^{K} k A_k (t - t_{j-1})^{k-1} \qquad (5)$$

Subtracting the approximated solution (Eq. 5) from the exact modified integrated point kinetics equation (Eq. 3) forms a residual $R(t)$. By means of the method of undetermined parameters [3] concisely written as:

$$\int_{t_{j-1}}^{t} V_r(t) R(t) dt = 0, \qquad r = 1, ..., K$$

one gets K algebraic equations (Eq. 6) to solve for the $A_1, ..., A_k$ parameters. The weighting functions $V_r(t)$ are unit step function over each subdomain:

$$V_r(t) = U(t) - U(t - t_r), \qquad r = 1, ..., K$$

where

$$t_r = t_{j-1} + \frac{t_j - t_{j-1}}{2^{r-1}}$$

Next, the aboved mentioned K algebraic equations are written:

$$\sum_{k=1}^{K} R_{rk} A_k = S_{rk} \qquad r = 1, ..., K, \qquad (6)$$

where:

$$R_{rk} = \Delta t_r^k - \left[\frac{\rho(t_{j-1})\Delta t_r^{k+1}}{k+1} + \frac{a_1 + 2a_2 t_{j-1})\Delta t_r^{k+2}}{k+2} + \frac{a_2 \Delta t_r^{k+3}}{k+3}\right]$$

$$- \sum_{i=1}^{m} \left\{ \frac{\beta_i'(t_{j-1})}{\Lambda(t_{j-1})} \frac{[\Delta t_r^{k+1} - (k+1) I_{i,k}(\Delta t_r)]}{k+1} \right.$$

$$\left. + (b_{1i} + 2b_{2i} t_{j-1}) \frac{[\Delta t_r^{k+2} - (k+2) I_{i,k+1}(\Delta t_r)]}{k+2} + b_{2i} \frac{[\Delta t_r^{k+3} - (k+3) I_{i,k+2}(\Delta t_r)]}{k+3} \right\}$$

and:

$$S_{rk} = \left(\rho(t_{j-1})\Delta t_r + (a_1 + 2a_2 t_{j-1}) \frac{\Delta t_r^2}{2} + a_2 \frac{\Delta t_r^3}{3} + \sum_{i=1}^{m} \left\{ \frac{\beta_i'(t_{j-1})}{\Lambda(t_{j-1})} [\Delta t_r - I_{i,0}(\Delta t_r)] \right.\right.$$

$$\left.\left. + (b_{1i} + 2b_{2i} t_{j-1}) \left[\frac{\Delta t_r^2}{2} - I_{i,1}(\Delta t_r) \right] + b_{2i} \left[\frac{\Delta t_r^3}{3} - I_{i,2}(\Delta t_r) \right] \right\} \right) A_0$$

$$+ \sum_{i=1}^{m} \left\{ \lambda_i \left[C_i(t_{j-1}) I_{i,0}(\Delta t_r) + \zeta_i(t_{j-1})\Delta t_r + (c_{1,i} + 2c_{2i} t_{j-1} \frac{\Delta t_r^2}{2} + c_{2,i} \frac{\Delta t_r^3}{3} \right] \right\} + Q(t_{j-1})\Delta t_r$$

The so called I functions are defined by:

$$I_{i,k}(\Delta t) = \int_{t_{j-1}}^{t} \exp[\lambda_i (t - t')](t' - t_{j-1})^k dt', \qquad \Delta t \equiv t - t_{j-1}$$

As can be seen above, R_{rk} and S_{rk} contain the rearranged physical parameters of the original point kinetics equations. The parameters are in general time dependent and as their functional dependencies cannot be prespecified, they are approximated by fitting to quadratic functions over the time intervals. S_{rk} includes the terms which are independent of the neutron concentration, among which is the external source which has a known constant value. K is chosen in SAS4A to be 2, since quadratic functions have shown to yield good accuracy in other codes, and they are well suited to be used in conjunction with the automatic time step selection technique of [2].

The above described technique is coded in subroutine "PKSTEP" of SAS4A. The mathematical activation of an external source becomes quite simple as it means only activating the appropriate term of the source in "PKSTEP" subroutine. One should only notice, the magnitude of this external source term

compensates the subcriticality of the core. So, the normalized power of the original critical core (usually 1) in the code SAS4A, has to remain constant after the core criticality is set below unity and the external source is activated. The point kinetics equation including an external source remains time independent and therefore gets its simplified form

$$N = \frac{Ql}{1 - k_{eff}} \tag{7}$$

where:
Q- external source strength
l- prompt neutron lifetime.

Practically, the steady state condition of ADS simulation within SAS4A code was achieved in the following process.
As the subroutine "PKSTEP" is not called in the steady state mode of the code, the first call to the transient part is initiated with a prompt negative reactivity jump, which sets K_{eff} to the desired subcriticality. Next, the amount of external neutrons is iterated until the normalized power level in the numerical calculation returns to its initial value (as mentioned before, it is usually 1). Due to the fact that a steady state phase is achieved in the transient part of the code slight discrepancies can occur from the expected normalized value. Such moderate fluctuations occur as a result of the immediate response of the reactivity feedbacks at each time interval. The prompt negative reactivity jump is not completely balanced by the external source and an artificial numerical reactivity feedback so it is quite natural introduced. This can cause fluctuations in the normalized power within the code. However, those discrepancies in the power level are negligible compared to the real physical effects which determine the power.

The above mentioned external source appears only in the point kinetics equation, so its entire contribution is to the amplitude function. The flux (power) spatial dependency on the source is excluded for the moment, due to its complexity (which will be described in chapter 2). Moreover, the code SAS4A actually separates the amplitude (power) function from the space dependency too, so it is quite natural to study the impact of the external source in the same manner, namely to leave out in the first step the spatial flux distribution recalculations. Nevertheless, the influence of the source location is handled later on, together with other core features which govern the flux (power) spatial distribution.

The spatial flux shape is linearly connected to the power distribution within the

core. As the main assumption in SAS4A is constant spatial shape of the flux during all the dynamic phenomena, it follows that the spatial power distribution is also steady. Thereafter all the fuel assemblies with approximately the same axial power distribution are represented by one fuel pin (and the corresponding coolant), which is called *Channel* in SAS4A. Each channel is weighted in accordance with the number of assemblies it represents. The total core power is normalized over all the channels needed to describe the assemblies. Each segment in the channel has a partial fixed weight, so in case of a change in the overall power amplitude level, the power spatial shape maintains always its original form.
The reactivity feedback coefficients during thermodynamic transients are currently evaluated (as the flux shape) by means of diffusion codes and are inserted as input data for SAS4A. As mentioned before the first order perturbation theory is used to determine the reactivity coefficients (based again on the constant flux shape assumption). Those calculated parameters together with the above described channel structure of the core, can be regarded as the prespecified spatial full neutronic kinetics of SAS4A.

2.2 Simulation of ADS with the SAS4A code

The primary objective of the ADS simulation was to verify whether activation or shutdown of an external source could be demonstrated without computational difficulties within the relevant subroutines. This includes mainly the code accuracy and stability after large reactivity insertion, during which a sudden change in the source strength should be possible.
Also important was to prove whether the overall effect of the external source (mainly concerning the power) is well presented within SAS4A.

The ADS simulation was demonstrated using Superphenix, sodium cooled model. The calculations of the flux and power distribution were those for a critical reactor and therefore the number of channels chosen and the reactivity coefficients could be different for an external source predesign. Nevertheless, for the purposes mentioned above this core presentation is sufficient. Thereafter the core configuration resembles an artificial source distributed over all the reactor. In such a way the flux shape with or without the external source is the same, and only the flux amplitude is enhanced by the external source. From a practical viewpoint this assumption is not realistic as any real external source will definitely distort the flux distribution. Yet the artificial spread source allows for the usage of a point kinetics model in the code and leads to the required comparison between critical assemblies and subcritical devices driven by an external source.

In order to understand the code response to the ADS characteristic phenomena, three basic types of incidents are demonstrated:
1. A moderate reactivity ramp of 0.15$/sec, which is simulation of control rods withdrawal.
2. A large unlimited reactivity ramp of 30$/sec.
3. A very large limited reactivity insertion of 170$/sec for a period of 15 msec.
The latter case was chosen to be compared with the test case carried out by Rubbia [4].

2.3 Results and conclusions

The results of the different cases are plotted in the following figures (1-6). All the tests were calculated up to the appearance of "pin failure" in one of the channels. This means fuel leaks through the molten cladding to the coolant. Once this phenomenon occurs, the SAS4A code subroutines fail to describe the mechanism of the phenomena correctly as they are not quite suitable for "pin failure" conditions in particular if ADS simulation is considered.

In order to overcome the problems connected with the sodium coolant in a fast reactor it was suggested by [4] to use lead as a coolant. The lead coolant possesses some advantages over the sodium coolant. It has lower absorption cross section, causes less moderation and so the energy spectrum is harder, leading to a remarkable lower reactivity void coefficients in comparison with sodium. Moreover lead has a significant higher boiling temperature. Well established data for lead are not available yet for the SAS4A code. Nevertheless, a preliminary test compares the reactivity feedback of the originally installed sodium coolant with a 'lead-like' void coolant reactivity. This is possible in SAS4A by reducing the multiplier "VOIDCOR" in the input, which is linearly connected to the void reactivity. All other thermal properties belong to Sodium. Thereafter, the results presented are only a first estimate of the effect of the reduced void reactivity of lead. For further research on the reactivity feedback, accurate lead properties should be implemented in SAS4A.

Fig. 1 shows the different void reactivity effect of the two coolants by inserting a reactivity ramp ($0.15\$/sec$). The lead-like coolant has lower positive void reactivity (compared to the Sodium coolant) and therefore "pin failure" occurs later. In severe accidents this could be of great importance. All the next graphs were also calculated with "lead-like" coolant.

Fig. 2 simulates ADS response to reactivity insertion. The initial subcriticality is $-5.5\$$ which means $K_{eff} \cong 0.98$. This value is momentarily the a reasonable upper value for an ADS and was used in all the next core simulation. The reactivity ramp in Fig. 2 is as in Fig. 1 namely $0.15\$/sec$ up to $3.5\$$, so the remaining subcriticality is $2\$$. The normalized power rises with the increasing reactivity and then stays steady, maintaining a power level which fits Eq. 7 for the case of a $2\$$ subcritical core driven by an external source. The other curve in Fig. 2 represents shut down of the source. In this case the power drops to a level comparable with a prompt jump approximation of the given $-2\$$. The mathematical formalism is given by Eq. 1 (the source excluded) which results in the expected decay heat phenomenon shown in Fig. 2.

The second transient tested is the core response to the insertion of an unlimited reactivity ramp of $30\$/sec$. Fig. 3 refers to the power excursion of the initial critical assembly while Fig. 4 represents an ADS with subcriticality of $-5.5\$$. The Doppler oscillations are well observed in Fig. 3 for the initially critical case. Inserting the same ramp within a subcritical system, leads to a power gradient, as long as K_{eff} is below unity (Fig. 4).
After $183ms$ the core becomes supercritical and the existence of the source suppresses the Doppler oscillations and the normalized power rises steadily, until "pin failure" occurs. If the source is shut down before supercriticality is reached, about $50ms$ can be gained before the power rises sharply. Later on, as the core is in a supercritical phase, the same pattern of the power excursion in a critical mode (Fig. 3) repeats itself. Interesting is the time to pin failure in this case. Even if the source is shut down the failure occurs almost at the same time as in the case where the source is "on" during the entire incident. Moreover when the external beam is removed the power reaches higher levels during the transient compared with the the case in which the source is "on". This is attributed to the enhanced Doppler effect in the system without the external source.
Consequently, from the phenomena shown in Fig. 4 the importance of the source concerning reactivity incidents, is valid if the core remains subcritical. Once the core becomes critical the existence of a source has a negligible effect on the safety analysis of the core. Nevertheless, it will be later shown that the source does influence the core multiplicity (which replaces K_{eff} in a source problem) through its location within the system and so has an impact on the reactivity too. This later effect reflects the distorted flux shape which governs the leakage rate and the enhanced $\Sigma_{n,2n}$ reaction rates in the vicinity of the source. However, as the calculations described so far are based on point kinetics model exclude any spatial phenomenon, the impact of the source location is not yet integrated in the code. Thereafter, the plots presented in this section are limited in their ability to demonstrate the full transient phenomenon. The conclusions regarding the source shut down could be different, as an increase or decrease in the criticality (following the shutdown) is expected, depending on the source location, the

energy spectrum of the source and the isotopes concentration in each subassembly.

The third incident evolves the insertion of $170\$/s$ for a limited time of 15 ms. The subcriticality is as before $K_{eff} \cong 0.98$. This case emphasizes the main difference between ADS and critical systems. The power of the critical system rises sharply corollary to the immense reactivity jump (Fig. 5) while the power of the ADS system rises quite slowly (Fig. 6) as long as the system remains subcritical, and after 15ms stabilizes on a new level (in accordance with Eq. 7). Shutting down the source leads as in the former cases to the expected slowly decaying power. The curve in Fig. 5 was compared with [4]. The peaks of the critical systems in [4] were lower by more than one order of magnitude. Although point kinetics tends to overestimate the power such large differences seem to be excessive. Other comparisons with [5] confirm the results obtained by the SAS4A runs. On the other hand, results concerning the power level in the transient state (Fig. 6), are in agreement with [4]. However the moderate slope of the curve in [4] for the power decrease after shutting off the source is not clear, since shutting down the source should lead to a sharp power decrease.

Based on the three examples, SAS4A can, in principle, handle an Accelerator Driven System as well as a critical fast reactor. Nevertheless the implicit basis of SAS4A which assumes constant flux shape and well estimated reactivity feedback coefficients (along the whole transient) has to be verified for ADS where the flux shape is more sensitive to local perturbations. Moreover, the criticality of the core depends also on the source location and to some extent on the emission energy spectrum of the spallation target.

The modification needed and the problems connected with specifying ADS feedback coefficients for SAS4A code, are discussed in the next chapter.

3 Perturbation theory considerations for ADS

The neutronic input data for SAS4A contains reactivity feedback coefficients for reactor material and density perturbations. Those perturbations are expressed through:
1. fuel Doppler feedback reactivity
2. fuel and cladding axial expansion feedback reactivity.
3. coolant density feedback reactivity
4. coolant void feedback reactivity
5. core radial expansion feedback reactivity
The above feedback coefficients are tabulated for each segment in each channel input block (called "POWINC" in the input data of SAS4A).

The procedure for establishing the reactivity feedback coefficients is based on the modular code package KAPROS [6], developed at FZK. The first code module KARBUS [6] evaluates the macroscopic cross sections of the isotopes in the core, for each relevant temperature and density. The present study utilizes a group constant library similar to the 69 energy group structure of the WIMS system [11]. For the 3-dimensional time-consuming flux calculations with D3E [7], it is customary to collapse the cross-sections into a coarse group structure usually by means of standard collapsing procedures [6].

Once the flux distribution is calculated and using the known cross sections, the power distribution in the core is determined. All the fuel pins with approximately the same power distribution are collapsed into one representative channel. This channel includes the fuel pin and its surrounding coolant. The relevant reactivity coefficients are calculated for each segment of the mentioned channel, by means of another program belonging to KAPROS package, called AUDI3 [19]. One application of this program makes use of first order perturbation theory and calculates all the reactivity coefficients. This is done for all the channel segments relative quickly as only the unperturbed flux is needed. Finally a special routine re-organizes the data to a form which can be read by the code SAS4A.

The basic assumption in SAS4A is the constant flux distribution during transient processes. In fast critical reactors with a "usual" radial Bessel function flux distribution, local perturbations have indeed minor effect on the overall flux. If the flux shape is governed by an external source the flux tends to have a decaying exponential (for a non multiplying, non absorbing medium) shape which can be significantly distorted by small amount of fissionable or absorbing isotopes. Consequently, the flux distribution is expected to be more sensitive to local perturbations in ADS and in particular, the flux in the near vicinity of the source.

A study done by [8] gives a first estimate to the sensitivity of the ADS flux depending on different subcriticality levels. Fig. 8 shows the results of this investigation. The flux peak is decreased by about 10% for a 1% increase in K_{eff} in the very near vicinity of the source (left edge of zone 1, Fig. 9). Away from the source (zone 2, Fig. 9) the flux dependence on the subcriticality is of minor importance. Consequently, the curves in Fig. 8 indicate that the assumption of constant flux distribution in SAS4A should be modified. For small perturbations a quasi static approach might be used in which the flux shape (and therefore the power distribution) is modified in the various channels, depending on the maximum allowed error in the flux.

A further important issue is the validity range of first order perturbation theory. The reactivity changes within the core are basically dependent on two thermal phenomena, temperature and density changes. The former change has an impact mostly on absorption rate and the latter on scattering and leakage rates. In order to assess the validity of the first order perturbation theory, an ADS core design (Fig. 7) was tested with the KAPROS codes Package [6,7]. The core is made up of 7 hexagonal rings around the center subassembly (No. 1 in Fig. 7) where an external source could be inserted. The first ring around the center contains only lead coolant . Surrounding it, are four rings of natural uranium mixed with Plutonium 239 fuel with lead coolant and other Plutonium isotopes to be incinerated (see section 2.3). Those rings have a reflector at the top and bottom of the fuel, where the coolant replaces the fuel. The sixth ring is a blanket and the seventh is again coolant. Two cases were analyzed using the same core configuration just described. The first is the source-free (homogeneous) problem and the second case the inhomogeneous problem with a central external source. The importance of checking also homogeneous cases is twofold. First, the code should respond accurately when the source is shut down. Second, the different configuration of an ADS without fuel in the center zone, leads to strongly space dependent feedbacks.
The results of this analysis is presented in the next section.

3.1 Validation of first order perturbation theory

The reactivity feedback coefficients which appear in POWINC input block data, are usually based on first order perturbation theory. As the intention of the current research is to use SAS4A code also for ADS where the application of first order perturbation theory is questionable, it is first worthwhile to study the characteristic of eigenvalue problems in connection with perturbation theory. It will serve as a benchmark case against which perturbation theory for ADS can be analyzed. This section re-examines the efficiency and accuracy of perturbation theory for eigenvalue problems. The next sections looks for the possibility of adapting perturbation theory also to ADS simulation.

In order to estimate the accuracy of perturbation theory for eigenvalue problems, a first order perturbation calculation was compared with an exact perturbation theory treatment, and with an exact solution as well. In the latter case K_{eff} is calculated directly twice, with and without perturbation, and the difference of the values of $1/K_{eff}$ is used to evaluate the reactivity feedback. The computations were carried out with the code D3E [7] for direct criticality evaluations and with the code AUDI3 [19] for perturbation theory. The homogeneous equation from which K_{eff} is calculated is based on describing the multiplicity of the core using the diffusion eigenvalue equation:

$$M\Phi \equiv \nabla \cdot D(r)\nabla\Phi(r) + \Sigma_a(r)\Phi(r) = \frac{1}{k}\nu\Sigma_f(r)\Phi(r) \equiv \frac{1}{k}F\Phi \quad (8)$$

where
D - diffusion coefficient.
Σ_a- macroscopic absorption cross section
$F \equiv \nu\Sigma_f-$ production operator
M - destruction operator (leakage plus absorption)
k - eigenvalue and k_{eff}

The numeric computation was done separately for each kind of disturbance. This is in accordance with the linearity of the reactivity feedback contribution in SAS4A code.
The results of reactivity feedbacks following a temperature decrease from $1183K$ to $300K$ are shown in table 1. The perturbed SA's- SubAssemblies- referring to Fig. 7, are indicated in the first column of the table. The $300K$ was chosen

because of the enhanced Doppler effect at low temperature, so that the first order perturbation theory is evaluated also for relatively large perturbation. Yet one should bear in mind that this temperature decrease is only an artificial example and is not a realistic case, as the melting point of lead is around $600K$.

Perturbed SA's	1^{st} order perturbation	exact perturbation	exact solution	multi-plicity
$8-37$	$2.1826E-03$	$2.2540E-03$	$2.2541E-03$	–
$20-37$	$1.0472E-03$	$1.0646E-03$	$1.0644E-03$	–
$38-61$	$8.8194E-04$	$8.9627E-04$	$8.9612E-04$	–
$62-91$	$5.6889E-04$	$5.8196E-04$	$5.8192E-04$	–

Table 1: Reactivity feedbacks for temperature decrease from 1183 K to $300K$, for a source free core.

From table 1 it is seen that first order perturbation leads to results close to the exact (direct) solution for temperature disturbances, even at relative large reactivity feedbacks of about 0.6\$.

Next, the fuel zone density is perturbed. First, the impact of density changes in the coolant are analyzed. Then, diluted fuel due to expansion of the rods are examined. Both tests are done by perturbing the two inner rings which contains fuel (SA's 8-37 in Fig. 7).

Table 2 refers to void perturbations in the coolant of the fuel zone. Table 3 refers to density perturbations due to expanded fuel.
Table 3 and the lower part of table 2 simulates pin fuel expansion, at the first

Lead void fraction (α)	1^{st} order perturbation	exact perturbation	exact solution	multi-plicity
0.5	$-5.6770E-03$	$-3.1679E-03$	$-3.1624E-03$	–
0.25	$-1.7867E-03$	$-1.2680E-03$	$-1.2642E-03$	–
0.09	$-0.4555E-03$	$-0.3952E-03$	$-0.3925E-03$	–
.04	$-1.7927E-04$	$-1.6773E-04$	$-1.6666E-04$	–
.02	$-8.5205E-05$	$-8.2355E-05$	$-8.2355E-05$	–

Table 2: Void Reactivity feedbacks in the coolant in SA's $8-37$, for a source free core.

stage of power excursion.

Partial fuel volume	1^{st} order perturbation	exact perturbation	exact solution	multi-plicity
0.98	$-5.7855E-03$	$-5.7671E-03$	$-5.8762E-03$	–
0.96	$-1.1662E-02$	$-1.1587E-02$	$-1.1847E-02$	–
0.92	$-2.3322E-02$	$-2.3020E-02$	$-2.2405E-02$	–

Table 3: Reactivity feedbacks of density decrease in fuel SA's $8-37$, for a source free core.

The given reactivity feedbacks in table 3 verify the accuracy of first order perturbation theory.
Table 2, confirms the accuracy of first order perturbation theory up to about $\alpha = 0.05$. At higher voids (from $\alpha = 0.08 - 0.09$) the deviation of first order perturbation theory is well noticeable. The reason for the deviations is the reduced number of scattering collisions at large voids. Thus, the basic assumption of the first order perturbation theory is violated as the energy dependent perturbed flux differs significantly from its unperturbed shape.
In the first case of temperature disturbances or in the case of fuel expansion, mainly the absorption collisions are affected so the perturbations can be large, but the unperturbed energy dependent flux is only slightly biased. Consequently, the unperturbed flux is a good approximation for the perturbed flux and first order perturbation theory is applicable. In the case of density disturbances, the reduced scattering collisions distort the flux shape and first order perturbation theory is not recommended as is seen from the poor accuracy for higher voids, in table 2.

The multiplicity factor column added in the above tables is actually the alternative way of measuring K_{eff} for source free systems. This factor is calculated by dividing neutron production by neutron losses. In homogeneous (eigenvalue) problems, it is self evident, as the production operator and the destruction operator is equal to the value of K_{eff} resulting from the mathematical solution (Eq. 8). In source problems, there is no eigenvalue solution. Instead, the existence of the source expresses the difference between the losses rate of neutrons in the core ($M\Phi$ in Eq. 8) and the production rate ($F\Phi$ in Eq. 8). Therefore, if one is interested in the multiplicity of inhomogeneous assemblies, it is necessary to calculate explicitly all the terms contributing to the production rate and the losses rate from which the multiplicity factor G is uniquely defined. The G factor replaces the eigenvalue K_{eff} of homogeneous problems (see chapter 4). The calculation of the multiplicity factor is sometimes complicated, in particular due to the difficulties of exact leakage estimation at the core boundaries where some diffusion solution methods lack the needed numeric scheme. In particular, no data are given for the multiplicity factors in the above tables, as the code AUDI3 [19] (which is used to transfer data to SAS4A code)

cannot handle yet the leakage term appropriately. Still the factor is mentioned in the tables to stress out its importance for source problems and to indicate the code AUDI3 cannot be used for source cases as long as it is not verified against the eigenvalue of homogeneous problems. In the meantime the correct leakage term, has reached its final validation stage in D3E/D3D/AUDI3 codes. Other codes (DIXY2 ,CITATION) compute the leakage term appropriately, and were verified by comparing the multiplicity factor with the eigenvalue in a benchmark homogeneous problem, which means that both factors were equal (see chapter 4).

3.2 Difficulties using perturbation theory in inhomogeneous problems

The previous section dealt with first order and exact perturbation theory and their validity range for critical assemblies. In inhomogeneous equations the flux term is even more sensitive to local disturbances so the former procedure for developing perturbation theory should be revised and modified. Moreover several parameters, which were relatively easily defined and evaluated for eigenvalue problems, are not applicable for external source problems and alternative solution techniques should be developed.

To begin with it is desirable to revise the definition of an adjoint flux. The adjoint flux can be evaluated for homogeneous problems by just writing the operators of Eq. 8 in their adjoint form, and solving this equation with the same method used for the real flux equation.
In inhomogeneous problems the governing equation differs from the homogeneous one by a new term, the external source, which replaces mathematically the K_{eff}, and thus maintaining balance between neutron losses and production.
This means Eq. 8 is modified to:

$$(M - F)\Phi = Q \tag{9}$$

Q is the external source neutron rate and the other terms are the same as in Eq. 8.
The real flux is computed iteratively from Eq. 9, but without eigenvalues, so it follows there is no way to define K_{eff} for the system. Therefore, the multiplicity

factor is the only direct way to calculate the reactivity feedbacks by comparing the unperturbed core with the perturbed one.
Another method to assess the reactivity feedbacks is to follow the homogeneous pattern to seek for a solution using methods based on perturbation theory. Those methods are well established for critical reactors[15], and are applied to SAS4A input data. For a source problem it is still necessary to have an adjoint flux for first order perturbation method.

The equation defining the adjoint flux for an external source system is:

$$(M^+ - F^+)\Phi^+ = Q^+ \tag{10}$$

where the symbols have the same meaning as in Eq. 9 and the $'+'$ sign indicates the adjoints forms of the relevant terms.

Eq. 10 includes a new term Q^+ which is the adjoint source. This term is not uniquely defined and can be arbitrarily chosen. In return, the adjoint flux (Φ^+) can get different values. But - for reactivity feedback evaluations - the value of the adjoint flux (function) has to be fixed. This implies the adjoint source should be determined and given only one value. A meaningful adjoint source is not possible yet since this adjoint term is based only on the mathematical consideration of Eq. 10. Nevertheless, some ideas could be proposed to specify the adjoint source with respect to known properties of the adjoint flux. For example, the definition of the adjoint flux as *importance* of a neutron within the homogeneous core, is based on taking the adjoint source as the cross section Σ_d characterizing an imagined detector placed in the core [16]. Another choice for the adjoint source is the fission cross section value in each segment as is suggested by [9]. This idea is also supported by variational methods considerations [10]. A questionable approach is the use of adjoint homogeneous flux for the solution of the inhomogeneous case. As can be seen, the drawback of the above examples is that the adjoint function (or adjoint source) for external source problems gets different values, usually depending on the certain property one is looking at.

The next section deals with the definition of perturbation theory, followed by a mathematical procedure, upon which a suitable adjoint function might be appropriate for the usage of first order perturbation method, concerning ADS simulations.

3.3 Formulation of perturbation theory for inhomogeneous problems

In order to analyze perturbation theory for ADS, it is suggested to start with the known eigenvalue method, and try to reproduce systematically the solution steps for inhomogeneous equations. Both procedures are based implicitly on the existence of a well defined stationary state. This assumption is yet to be proved for ADS. Yet, for the moment it is beyond the scope of this study.

The basic theory is regenerated in the following in a very simplified form namely only disturbances in the destruction term are accounted for the mathematical procedure. In this way the advantages of the homogeneous solution method over ADS solution procedure are well demonstrated. Nevertheless, the conclusions are valid also for perturbations in the production operator.

3.3.1 Perturbation theory for critical assemblies

Perturbation theory is based on using adjoint operators and adjoint functions. Therefore, it is useful to recall the definition of an adjoint operator.
An operator M^+ is defined as adjoint to an operator M if the following inner products are equal:

$$(M^+ f, g) = (f, Mg) = \int_V d^3r f^* Mg \tag{11}$$

for every f(r) and g(r) satisfying the boundary condition:
$f(r_{surface}) = g(r_{surface}) = 0$.
f^* denotes the complex conjugate of f(r).
An adjoint flux Φ^+ is defined for the eigenvalue problem, as the corresponding solution of:

$$M^+\Phi^+ = \frac{1}{K} F^+\Phi^+ \tag{12}$$

where M^+ is the adjoint destruction operator and F^+ is the adjoint production operator (based on the real operators in Eq. 8).

The basic equations for a homogeneous (eigenvalue) problem are reproduced. A perturbation δM is introduced in the destruction operator which leads to the equation:

$$M'\Phi' = \frac{1}{K'} F\Phi' \tag{13}$$

where $M' = M + \delta M$.
Taking the scalar product of Eq. 13 with the adjoint flux Φ^+ of Eq. 12 results in:

$$(\Phi^+, M\Phi') + (\Phi^+, \delta M\Phi') = \frac{1}{K'}(\Phi^+, F\Phi') \tag{14}$$

Based on Eq. 11, the scalar product of Eq. 12 with the perturbed flux $\Phi^{'}$ is written:

$$(\Phi^+, M\Phi') = (M^+\Phi^+, \Phi') = (\frac{1}{K}F^+\Phi^+, \Phi') = \frac{1}{K}(\Phi^+, F\Phi') \tag{15}$$

By subtracting Eq. 15 from Eq. 14, one gets:

$$-\delta\rho = \left(\frac{1}{K'} - \frac{1}{K}\right) = \frac{(\Phi^+, \delta M\Phi')}{(\Phi^+, F\Phi')} \tag{16}$$

This expression points out the merit of using adjoint operators and and their adjusted inner products. The perturbed and unperturbed criticalities can formulate an explicit expression for the reactivity feedback based on the disturbance in the destruction (in general also production) operator. The idea of "perturbation theory" comes in, by assuming small δM and therefore the flux perturbation $\delta\Phi = \Phi^{'} - \Phi$ is small. Consequently a series expansion of Eq. 16 is used and only the first order terms are kept. This leads to "first order perturbation theory", written as:

$$-\delta\rho = \frac{(\Phi^+, \delta M\Phi)}{(\Phi^+, F\Phi)} \tag{17}$$

Eq. 17 points out the advantage of first order perturbation theory. Only the unperturbed flux is used to define the reactivity feedback in case of changes in the destruction or production operators. For practical calculation this means considerable reduction in computation time, in particular when many feedback coefficients should be recalculated.

3.3.2 Applying the perturbation technique to ADS

Based on the homogeneous procedure the following approach is applied for source problems. Again, the perturbation δM is only in the destruction operator. The governing inhomogeneous equation is:

$$M\Phi = F\Phi + Q \tag{18}$$

and the equation for the perturbed core is written as:

$$(M + \delta M)\Phi' = F\Phi' + Q' \tag{19}$$

Several concepts can be suggested regarding the new mathematical constant Q'. If $Q' = Q$, the power of the perturbed system will differ from the unperturbed one (in accordance with Eq. 7). This will lead to different formulation than the one suggested below.
The preferable choice is to change the magnitude of Q' but not its location within the core. Thus, one can adjust the power to be the same as in the unperturbed equation (Eq. 18). The reactivity change will still depend only on the perturbation in the destruction operator. This option leads to a mathematical definition (Eq. 30) which introduces the differences between the inhomogeneous and homogeneous problem in a better visual manner. For the completeness of the discussion Q' could also be a new source in a new location. The procedure up to Eq. 30 is still valid. However, the new location contributes to variation in the reactivity. But, the basic idea in the following is to compare the same perturbation between a source free and an external source system. Therefore, additional contribution reactivity from the location of the source should be excludedi for the moment. Summarily, it seems useful and convenient to consider a source located in the same place and with intensity which maintains the same power of the unperturbed core.

Following the homogeneous solution technique for inhomogeneous equations, one writes the scalar product of Eq. 19 inserting an (arbitrary for the moment) adjoint flux Φ^+:

$$(\Phi^+, M\Phi') + (\Phi^+, \delta M\Phi') = (\Phi^+, F\Phi') + (\Phi^+, Q') \tag{20}$$

From Eq. 20, one can evaluate the multiplicity factor G for the specific ADS considered. This factor is the ratio of the neutrons production over neutron losses in the entire core. Actually it could be also written as:

$$\frac{F\Phi}{M\Phi} \rightarrow G \tag{21}$$

where $F\Phi$ is the production term and $M\Phi$ is the losses term. One should be aware not to confuse this expression with the homogeneous one. Here G is not

an eigenvalue and can only be obtained after the flux was determined by means of inhomogeneous solution methods. This means Eq. 21 is not a mathematical equation but rather a logical expression. The matrices F and M should be disintegrated to their local values: fission, absorption and leakage. Each local macroscopic cross-section is multiplied by the local flux and then the production terms and the absorption terms are summed separately. In addition, the flux shape of the source problem differs from the shape of the eigenvalue problem due to the strong dependency on the source location. Therefore, the multiplicity factor G is expected to be considerably different from the eigenvalue (criticality) of the homogeneous problem.
Next, in accordance with Eq. 18 an adjoint equation is defined:

$$M^{+}\Phi^{+} = F^{+}\Phi^{+} + Q^{+} \tag{22}$$

The scalar product of Eq. 22 is taken with the perturbed flux and by using the definition of Eq. 11:

$$(\Phi^{+}, M\Phi') = (\Phi^{+}, F\Phi') + (Q^{+}, \Phi') \tag{23}$$

Subtracting Eq. 23 from Eq. 20:

$$(\Phi^{+}, \delta M\Phi') = (\Phi^{+}, Q') - (Q^{+}, \Phi') \tag{24}$$

which can be reduced [16] to:

$$(\Phi^{+}, \delta M\Phi') = (\Phi^{+}, \delta Q) - (Q^{+}, \delta\Phi) \tag{25}$$

As the goal of this procedure is to find the reactivity feedbacks (based on perturbation theory), it is necessary to express the reactivity by means of the inhomogeneous equation variables. In the homogeneous solution this was self-evident (Eq. 17). For ADS, it is suggested to use the principle of Eq. 21 to define the reactivity of the inhomogeneous system.

The scalar product of Eq. 18 is taken with the adjoint flux Φ^{+} which yields an expression for the reactivity:

$$-\rho = \frac{(\Phi^{+}, Q)}{(\Phi^{+}, F\Phi)} \tag{26}$$

By rewriting Eq. 26 for the perturbed case and then subtracting from it the expression for the unperturbed case, one gets the reactivity feedback :

$$-\delta\rho' = \frac{(\Phi^+, Q')(\Phi^+, F\Phi) - (\Phi^+, Q)(\Phi^+, F\Phi')}{(\Phi^+, F\Phi')(\Phi^+, F\Phi)} \tag{27}$$

The numerator of Eq. 27 can be written in terms of unperturbed parameters and the perturbations:

$$-\delta\rho' = \frac{(\Phi^+, Q)(\Phi^+, F\Phi) + (\Phi^+, \delta Q)(\Phi^+, F\Phi) - (\Phi^+, Q)(\Phi^+, F\Phi) - (\Phi^+, Q)(\Phi^+, F\delta\Phi)}{(\Phi^+, F\Phi')(\Phi^+, F\Phi)}$$

from which:

$$-\delta\rho' = \frac{(\Phi^+, \delta Q)(\Phi^+, F\Phi) - (\Phi^+, Q)(\Phi^+, F\delta\Phi)}{(\Phi^+, F\Phi')(\Phi^+, F\Phi)} \tag{28}$$

Replacing the left parenthesis in the numerator, using Eq. 25:

$$-\delta\rho' = \frac{(\Phi^+, \delta M\Phi')(\Phi^+, F\Phi) + (Q^+, \delta\Phi)(\Phi^+, F\Phi) - (\Phi^+, Q)(\Phi^+, F\delta\Phi)}{(\Phi^+, F\Phi')(\Phi^+, F\Phi)}$$

Next, $\delta\Phi$ is replaced by $(\Phi' - \Phi)$ and the term (Φ^+, Q) is replaced by (Q^+, Φ). The latter change is based on the adjoint definition (Eq. 11) and is proved in [16]. Rewriting the latter equation again, forms an expression in accordance with exact perturbation theory:

$$-\delta\rho' = \frac{(\Phi^+, \delta M\Phi')(\Phi^+, F\Phi) + (Q^+, \Phi')(\Phi^+, F\Phi) - (Q^+, \Phi)(\Phi^+, F\Phi')}{(\Phi^+, F\Phi')(\Phi^+, F\Phi)} \tag{29}$$

One can continue with the same procedure (of a critical system) for deriving a first order perturbation theory equation. This will mean to expand the homogeneous equation terms into series and leave higher orders (than one) out. This procedure replaces the perturbed flux Φ' by the unperturbed flux Φ but here there are also terms including $\delta\Phi$ which can not be canceled. The equation is:

$$-\delta\rho = \frac{(\Phi^+, \delta M\Phi) + (Q^+, \delta\Phi) + \rho(\Phi^+, F\delta\Phi)}{(\Phi^+, F\Phi)} \tag{30}$$

The latter expression is similar to Eq. 17 for critical system but with two additional terms. Those terms are of first order and could contribute considerably

to the reactivity feedback. On the other hand they might cancel each other. Moreover, Eq. 22 cannot be solved as there are two unknown vectors Φ^+ and Q^+. It is clear that more knowledge is needed regarding the adjoint source Q^+ and the adjoint flux Φ^+. However, a straightforward method for evaluating the adjoint flux and source does not exist. The mathematical problems concerning such a method are discussed in the following, bearing in mind the solution trials presented in section 3.2.

3.3.3 Possible evaluation of an adjoint flux for ADS

The adjoint function in ADS depends on the adjoint source which is not defined. One set of equations connecting the two functions is obtained from Eq. 22. In order to get a unique solution another set is needed. The physical definition of the homogeneous adjoint flux is based on inserting an external source which eventually leads to the expression:

$$\int_V d^3r\Phi^+(r)Q(r) = \int_V d^3rQ^+\Phi(r) \tag{31}$$

For homogeneous problems one specifies a unit source for $Q(r)$ and in addition $Q^+(r)$ is chosen as the cross section $\Sigma_d(r)$ characterizing an imagined detector placed in the core. For ADS the considerations are different. The system is subcritical and the source governs too the flux distribution. This means that the adjoint flux is influenced by the source. It follows that the adjoint source depends on the source itself. In return this means Eq. 31 does not provide a set of equations but only one condition to be fulfilled. This aspect differs from the homogeneous adjoint definition.

The dependency shown between the two unknown adjoint vectors points out the necessity of a new set of equations in addition to Eq. 22. One can start with another condition based on the multiplicity factor G:

$$\frac{F^+\Phi^+}{M^+\Phi^+} \rightarrow G \tag{32}$$

The same consideration as for Eq. 21 are valid also here. Eq. 32 is therefore only a condition imposed on the solution of the adjoint flux but is not a method

to solve the adjoint function.

The above arguments emphasize the need of more knowledge concerning the adjoint source problem in order to solve the adjoint flux uniquely, as one is left with only one set of equations (Eq. 22) and two integral dependencies between the variables.

If one is interested only in the overall reactivity feedback and not in the local reactivity contribution, (using the basic idea of first order perturbations for all local disturbances together) a simpler approach is suggested. Eq. 26 can be rewritten for the perturbed case:

$$-\rho' = \frac{(\Phi^+, Q')}{(\Phi^+, F\Phi')} \tag{33}$$

Dividing now Eq. 33 by Eq. 26 and rearranging the equation gives:

$$\rho' = \frac{Q'}{Q}\rho \tag{34}$$

Eq. 34 is a very simple special case which allows for reasonable results with the available codes. The simplicity is based on the following assumptions:
1. The perturbed flux is approximated by the unperturbed flux.
2. A source located at only one point in the core, is considered. So the same one value of the adjoint flux appears in the denominator as well as in the numerator, and is reciprocally canceled. Thereafter, only the strength of the source remains in the equation. Furthermore, Eq. 34 implicitly indicates that all the neutrons emitted from the spallation target are with energy belonging to only one energy group. This is not in general the case, so in realistic cases the full calculation of the adjoint (weighting) function is inevitable. Nevertheless, in the example shown in table 4 it was assumed that all the induced spallation neutrons do come from the highest group. The assumption reduces the computation considerably and enables the validation of the new developed scheme.

The verification of Eq. 34 was done by comparing it with exact calculation of the reactivity feedback for the perturbations indicated in table 4 in zone 2 of Fig. 9 as well as in the outer fuel zone of the core (zone 1 in Fig. 9). The exact calculation is done by calculating the perturbed reactivity and subtracting the unperturbed reactivity from it. All the results presented in this section were performed with the code DIXY2[14] which was verified for ADS calculations (see chapter 4).

Perturbation description	Exact calculation	Solution of Eq. 34	error (%)
$1183K \rightarrow 300k$ zone 2	$1.59289E-03$	$1.62328E-03$	1.9%
$1183K \rightarrow 600k$ zone 2	$7.75832E-04$	$7.69510E-04$	0.81%
$1183K \rightarrow 900k$ zone 2	$3.02962E-04$	$3.19433E-04$	5.4%
$1183K \rightarrow 1600k$ zone 2	$-3.3109E-04$	$-3.2797E-04$	0.94%
$1183K \rightarrow 300k$ zone 1	$1.05161E-03$	$1.08136E-03$	2.8%
$1183K \rightarrow 600k$ zone 1	$5.06055E-04$	$5.18703E-04$	2.5%
$1183K \rightarrow 900k$ zone 1	$2.00828E-04$	$2.04452E-04$	1.8%
$1183K \rightarrow 1600k$ zone 1	$-2.0970E-04$	$-2.2314E-04$	6.4%
lead volume 0.8*nominal, zone 2	$-9.355E-04$	$-7.241E-04$	22.6%
lead volume 0.8*nominal, zone 1	$-8.029E-03$	$-8.812E-03$	9.75%
lead volume 0.91*nominal, zone 2	$-3.8500E-04$	$-3.9586E-04$	2.8%
lead volume 0.91*nominal, zone 1	$-3.500E-04$	$-3.5521E-04$	1.4%
fuel volume 0.975*nominal, zone 2	$-5.1031E-03$	$-5.2746E-03$	3.3%
fuel volume 0.975*nominal, zone 1	$-4.3537E-03$	$-4.4844E-03$	3.0%

Table 4: Comparison of reactivity feedbacks of temperature and density changes in fuel zones 1 and 2 of Fig. 9. Convergence criterion: $1.E-05$. A central source core is considered.

The evaluated errors in table 4 are in general within the expected accuracy of first order perturbation theory (As Eq. 34 is based on the unperturbed flux appearing in the denominator of Eq. 33). Yet, for large coolant voids in the vicinity of the source the reactivity estimations are poor because of strong distortion of the flux.

In summary, the results in table 4 support to some extent the validity of the procedure developed in this section. More tests with realistic energy spectrum should be performed before drawing general conclusions. However, this should evolve explicitly the adjoint flux of an ADS and as mentioned above this function is yet to be defined.

Another aspect rising from table 4 is that one can calculate the multiplicity of a system without explicitly using the leakage term. This is useful by some numerical codes which fail to calculate explicitly and correctly the losses terms at the core boundaries , but still estimate the flux shape correctly.

At last it should be noticed that Eq. 33 is actually an extended version of Eq. 7 but expressed differently. In Eq. 7 the relation between the core power, the strength of the source and the criticality are explicitly demonstrated. In Eq. 33 the new reactivity is expressed by the change of the source term in

the numerator while the denominator is kept constant. This of course is only a mathematical way to find the reactivity of the perturbed core. In reality, changing the strength of the source has no impact on the reactivity and only manipulates the power level. This is corollary of the independency of the source strength and the reactivity.

4 Exact reactivity calculations for ADS

As mentioned in chapter 3 direct evaluation of the criticality for ADS is not possible as the solution method has no eigenvalue. Thereafter a logical substitute is defined namely the multiplication factor G which is the production rate over the losses rate. The multiplicity factor is, of course, valid for source free systems where it is identical with the eigenvalue (K_{eff}). Consequently, the verification of suitable codes for ADS simulation is performed by comparing the multiplicity factor with the mathematical eigenvalue k of a source free benchmark solution. If the two are identical, the specific code can be used for ADS calculations. Problems in evaluating the multiplicity factor mainly arises due to the leakage rate calculation. The leakage rate being a part of the losses term is proportional to the outward gradient of the flux (current) near the core boundaries. It appears that some codes cannot handle correctly this derivative. The problem lies usually by the definition of the meshes (point meshes, volume meshes etc.) and in particular at which point the derivative is estimated between two mesh points. This chapter deals with codes validated for source problems, so the multiplicity factor and in particular the leakage term are accurately calculated. In such a way, the impact of the source on the core criticality is well demonstrated and conclusions concerning the optimal core configuration are derived for ADS.

It is important to note that the multiplicity factor G for source problems is different from K_{eff} of the source free system only if the core is subcritical. Yet, the multiplicity factor of an ADS converges to K_{eff} if the two values approach one (Fig 11). Above one, the multiplicity factor is equal to K_{eff} and have no direct influence on the core criticality (except of minor effect through the spallation spectrum). This is in full agreement with the "usual" eigenvalue formalism of supercritical cores.

4.1 The effect of an external source on reactivity

The existence of the source in the core evolves two aspects which affect the criticality of the system. They are: the location of the source and to some extent the neutron emission spectrum. To quantify those effects a code which can evaluate properly the multiplicity factor of an ADS is needed. The diffusion code DIXY2 [14] estimates accurately the multiplicity factor and therefore is used here for the analysis. The applied cross section sets for the code are well validated for a broad range of application from thermal to fast systems [6].

The hard spectrum of the external source induces small changes through the (n,2n) reactions and is discussed first. The $\Phi\Sigma_{n,2n}$ is of the order of only half percent of the total neutron production rate for the current lead

cooled system. In the multigroup formalism of the KAPROS system the (n,2n) processes are treated as a negative contribution to the absorption cross section ([6]). This kind of treatment is consistent with eigenvalue calculations, and simplifies considerably the computational effort. For critical assemblies the error introduced by solving numerically the above system, was found to be negligible. For ADS simulation this error is expected to be also small.

Concerning the energy spectrum, tests done by [6] confirm that a false fission spectrum leads to considerable errors in the criticality evaluations. An iteration process improves the results. In the current calculation such iterations were done to increase the reliability of the calculated data. The spallation source spectrum is taken into account separately by input specifications in the flux calculations codes D3E,DIXY2,CITATION. The applied approximation considers a space independent distribution with 90% in the first energy group and 10% in the second energy group for all the collapsed group systems investigated in the current study (section 4.2).

The main influence to the reactivity comes from the location of the source. To quantify this effect the code DIXY2 was chosen. The core design is adjusted to the R-Z version with azimuthal symmetry for 3-D simulation. The core configuration is plotted in Fig. 9. The relative error of the code was assessed by comparing eigenvalues with multiplicity factors (production rate over losses rate) of source-free problems. Furthermore the code was also validated against another FZK diffusion code called D3D [7]. The comparison was performed by imposing a temperature decrease from 1183K to 600k in zone 2 of the core (Fig. 9). The reactivity feedbacks and the K_{eff} following such a disturbance were calculated using different methods. The materials used for the fuel zone are listed below and are based also on the idea of high level waste incineration.

MATERIAL-DENSITIES IN THE FUEL-ZONE (atoms/(barn*cm))

FUEL-PIN (at 1183K)	COOLANT (at 879K)	CLAD (at 879K)
'U 235 ' 9.9857E-05	'PB ' 2.9922E-02	CR 1.5030E-02
'U 238 ' 1.3408E-02		FE 5.8894E-02
'PU238 ' 2.2850E-05		NI 1.1928E-02
'PU239 ' 4.4087E-03		
'PU240 ' 1.4168E-03		
'PU241 ' 1.5545E-04		
'PU242 ' 9.8630E-05		
'AM241 ' 2.0810E-04		
'O ' 3.9637E-02		

parameter compared	perturbation: 600K in fuel zone 2	
	D3D(RZ)	DIXY2
REF: K_{eff} unperturbed	0.96767	0.96767
REF: G unperturbed	—	0.96691
K_{eff} perturbed	0.96867	0.96867
G perturbed	—	0.96792
$\delta\left(\frac{1}{K_{eff}}\right)$	$-1.0719E-03$	$-1.0711E-03$
$\delta\left(\frac{1}{G}\right)$	—	$-1.0807E-03$
1^{st} order perturbation	$-1.0544E-03$	$-1.0544E-03$
Exact perturbation	$-1.0722E-03$	$-1.0721E-03$

Table 5: Reactivity feedback and K_{eff}, comparing eigenvalue versus multiplicity factor G, for a homogeneous problem, using DIXY2 and D3D codes. The temperature decrease is from 1183K (reference) to 600K in fuel zone 2 (Fig. 9).

FUEL CHARACTERISTICS

Oxide density = 8.8958 g/cm**3
Heavy-Metal density = 7.8431 g/cm**3
HM atomic number density = .019819 atoms/(barn*cm)
PUfiss/HM mass ratio = 24.153 %
Fissile/HM mass ratio = 24.650 %
PU/U mass ratio = 46.994 % ; PU/U number-of atoms ratio= 46.718 %
Ufiss/U mass ratio = .7300 % ; PUfiss/PU mass ratio = 75.550 %

The blanket of the core (Fig. 9) contains pure Uranium with 0.25% $U235$ fraction.

The results shown in table 5 confirm the reliability of the DIXY2 code. In particular the multiplicity factor G diverges from the exact K_{eff} (of the source free problem) by less than 0.1% which is satisfactory. After validating the multiplicity calculation by DIXY2 the criticality dependency on the source location was examined. The source was located in three different places and its multiplicity factor was compared against the criticality of the same core excluding the external source.
The following results were obtained:

- Multiplicity of the source free core (homogeneous problem) $K_{eff} = 0.96691$
- The source located in the core center (Fig. 9). The multiplicity calculated: $G = 0.97631$

- The same source, located at point 'B' (Fig. 9). The multiplicity calculated: $G = 0.91141$
- The same source, located at point 'C' (Fig. 9). The multiplicity calculated: $G = 0.81321$

The different values of G emphasize the significance of the location of the source on the multiplicity factor. It is clear, a central source is the best way to get a negative reactivity feedback, by shutting off the source. On the other hand, a central source causes a very high peak factor in its vicinity. This means an optimization process should be performed to find the favorable core configuration.

Next the reactivity feedbacks of the source free core are compared against the source problem. Several possible disturbances are treated in fuel zone 2 (Fig. 9). One group of disturbances is temperature changes which have mainly impact on the absorption rate. Other possible incidents are voids in the lead coolant which reduce mainly the scattering rate (and therefore the leakage rate), and fuel expansion which reduce the absorption rate considerably with minor effect on the scattering rate.

In table 6 the differences between the reactivity feedbacks in a source-free core and in an ADS (central source, see Fig. 9)- undergoing the same perturbations in fuel zone 2 (Fig 9)- are presented. The results indicate the influence

Change description in Fuel zone 2	Reactivity feedback	
	Sourceless core	Central source
$\Delta T : 1183K \rightarrow 300k$	$2.223E-03$	$1.619E-03$
$\Delta T : 1183K \rightarrow 600k$	$1.080E-03$	$7.778E-04$
$\Delta T : 1183K \rightarrow 1600k$	$-4.596E-04$	$-3.242E-04$
$\Delta\rho$:-9% of coolant	$-3.257E-04$	$-3.334E-04$
$\Delta\rho$:-20% of coolant	$-9.587E-04$	$-9.412E-04$
$\Delta\rho$:-2.50% of fuel	$-7.159E-03$	$-5.131E-03$
$\Delta\rho$:-3.75% of fuel	$-1.079E-02$	$-7.749E-03$

Table 6: Reactivity feedbacks for temperature or density changes in zone 2 of Fig. 9. Convergence criterion: $1.E-04$.

of the existing source on the magnitude of the reactivity feedbacks during a postulated incident. If the temperature rises the central source core exhibits a smaller reactivity feedback in comparison with the source-free core. The same pattern is repeated for fuel expansion. For the coolant density decrease, the reduction (if at all) in the feedback coefficient for ADS is not significant in the

outer fuel zone. Yet a noticeable difference in the reactivity feedback for coolant void disturbances in the inner fuel zone can be seen in table 7. In this zone the scattering processes are less pronounced for ADS, as the hard spectrum of the source reduces the overall flux sensitivity to coolant void perturbation.

Change description in Fuel zone 1	Reactivity feedback	
	Sourceless core	Central source
$\Delta T : 1183K \rightarrow 300k$	$1.504E-03$	$1.051E-03$
$\Delta T : 1183K \rightarrow 600k$	$7.239E-04$	$5.060E-04$
$\Delta T : 1183K \rightarrow 1600k$	$-3.032E-04$	$-2.097E-04$
$\Delta\rho$:-9% of coolant	$-4.984E-04$	$-3.350E-04$
$\Delta\rho$:-20% of coolant	$-1.144E-02$	$-8.029E-03$
$\Delta\rho$:-2.50% of fuel	$-6.251E-03$	$-4.377E-03$
$\Delta\rho$:-3.75% of fuel	$-9.412E-03$	$-6.592E-03$

Table 7: Reactivity feedbacks for temperature or density changes in zone 1 of Fig. 9. Convergence criterion: $1.E-04$.

From the results shown in this section it is evident that the source existence and the initial energy spectrum of the spallation target distort the flux distribution and thereafter affect the multiplicity of the subcritical core. In particular it is important to note that shutting off the central source introduces a fairly large negative reactivity feedback, depending on the magnitude of the subcriticality of the source free case (see also Fig. 11). On the other hand, incidents occurring while the central source is still "on" reduce to some extent the expected negative reactivity feedback. This means the key point for safety analysis of ADS with a central source is the reliability of shutting down the source. For other source locations individual safety analysis is essential.

The above conclusions emphasize that modifications including different core configuration and reactivity feedback coefficients, are inevitable for ADS transient simulation. This is possible to do within the restart option of SAS4A.

4.2 The influence of numbers of energy groups on criticality calculations

All the results shown so far, using DIXY2 code, where carried out with four energy groups. Those groups were collapsed from the 69 "WIMS[11]" group structure, using standard collapsed procedures with fundamental mode calculations [6]. The energy boundaries of the groups are:
1. 10 MeV - 1.353 MeV
2. 1.353 MeV - 0.111 MeV
3. 0.111 MeV - 367.262 eV
4. 367.262 eV - 0.001 eV

In order to assess the accuracy of the former and future reactivity calculation some tests were recalculated with 10 and 16 energy groups. In the four group structure the main contribution to the fast fission spectrum comes from the three upper broad group (the fourth group contributes only 1% to the fission). For the ten and sixteen groups the last group starting at 367.26 eV was unchanged and 9 (or 15) groups were created from $10MeV - 367.26\ eV$. The energy groups for the ten groups structure and the sixteen groups structure are as follows:

10 group structure	16 group structure
1. 10.00 - 3.679 MeV	1. 10.00 - 3.679 MeV
2. 3.679 - 1.353 MeV	2. 3.679 - 2.231 MeV
	3. 2.231 - 1.353 MeV
3. 1.353 - 0.821 MeV	4. 1.353 - 0.821 MeV
4. 821.0 - 302.5 KeV	5. 0.821 - 0.500 MeV
	6. 500.0 - 302.5 KeV
5. 302.5 - 111.0 KeV	7. 302.5 - 183.0 KeV
	8. 183.0 - 111.0 KeV
6. 111.0 - 67.34 KeV	9. 111.0 - 67.34 KeV
7. 67.34 - 24.78 KeV	10. 67.34 - 40.85 KeV
	11. 40.85 - 15.03 KeV
8. 24.78 - 5.530 KeV	12. 15.03 - 9.118 KeV
	13. 9.118 - 5.530 KeV
9. 5530. - 367.3 eV	14. 5.530 - 2.239 KeV
	15. 2239. - 367.3 eV
10. 367.3 - 0.001 eV	16. 367.3 - 0.001 eV

parameter checked	10 Energy Groups		16 Energy Groups	
	no source	Central source	no source	Central source
G	0.96331	0.97424	0.96346	0.97430
$1183K \rightarrow 300k$	$2.193E-3$	$1.521E-3$	$2.178E-3$	$1.520E-3$
-20% of coolant	$-1.158E-3$	$-1.084E-3$	$-1.168E-3$	$-1.094E-3$
-3.75% of fuel	$-1.064E-2$	$-7.510E-3$	$-1.058E-2$	$-7.486E-3$

Table 8: Comparison of Multiplicity- G (equal to K_{eff} for source free core), and Reactivity feedbacks between calculations with 10 and 16 energy groups for perturbations in fuel zone 2 (Fig. 9). Convergence criterion: $1.E-04$.

By comparing table 8 with the former section (four energy groups), the results using four energy groups are in general quite sufficient for the basic studies in this chapter. For example, by shutting off the source, the negative reactivity according to the four energy groups calculation is: 0.94% compared with the 1.084% obtained by the 16 groups calculation or the 1.093% by the 10 groups calculation. The discrepancies are even less pronounced for reactivity feedbacks. Yet, if very high coolant void are considered (which would usually not be the case for lead coolant) one should use more energy groups, in order to achieve the needed level of accuracy.

An additional feature to be considered is the energy spectrum of the spallation source. In the current calculations the energy of the neutron emerging from the spallation target was divided 90% in the highest energy group and 10% in the second group for all energy group combinations considered.

4.3 Full 3D hexagonal ADS simulation using CITATION code

The diffusion code CITATION [20] is widely used and has a large variety of core options. Among those exists the 3D hexagonal configuration, suitable for ADS design. The most important feature of the code in concern with the current work, is its ability to solve source problems, in particular to calculate correctly the leakage term. As already mentioned the code has numeric meshes which allow for exact derivation of the stream term at the boundaries of the system. After validating CITATION against D3E [7] code for source-free benchmark problems, some ADS configurations were analyzed. The basic ideas were already presented qualitatively by [21] but they lack the necessary accuracy of the results shown in this work.

4.3.1 ADS optimization by means of distributed sources

The original ADS - IAEA benchmark problem - is based on the proposal of [4] for an energy amplifier. It uses TH232 enriched with U233 (10%) as fissile material. This fuel has the advantage of not breeding plutonium and its successor long live radioactive actinides. In the following this fuel is used for the various simulations.
The fuel, coolant and clad isotopes densities are (atoms/(barn*cm)):

FUEL-PIN (at 1183K)	COOLANT (at 879K)	CLAD (at 879K)
'TH232' 1.9126E-02	'PB ' 2.9910E-02	'CR ' 1.0089E-02
'U 233 ' 2.1160E-03		'FE ' 7.5801E-02
'O ' 4.2485E-02		

FRESH-FUEL CHARACTERISTICS

OXIDE DENSITY = 9.316000 G/CM**3
HEAVY-MATERIAL DENSITY = 8.187214 G/CM**3
HM ATOMIC NUMBER DENSITY = .021243 ATOMS/(BARN*CM)

The motivation for new configurations instead of the original central source design [4] is corollary of the difficulties in removing the heat from the spallation target [22]. The solutions suggested to this problem mainly concentrate on improving the heat transfer near the target (for example by analyzing different materials from which the target is made). Along with the material research it was suggested by [21] to use a multiple source system which reduces the needed strength of each individual source and consequently the heat generated around each source will be proportionally reduced. This approach evolves also spatial effects concerning safety, operational and technical aspects of the core.

Three core configurations are analyzed:
1. A core with three sources, each of them surrounded by a lead ring, located in the mid fuel zones (Fig. 10).
2. A central source core located in subassembly -SA- 1 (Fig. 10) surrounded by a lead ring (SA's 2 to 7), and fresh fuel elements elsewhere (SA's 8 to 169).
3. Six sources located at the outer fuel subassemblies (SA's No. : 92,98,104,110,118,122 in Fig. 10), each of them surrounded by a lead ring made of six neighboring SA's. All the rest SA (up to 169) are as before loaded with the fresh fuel described above.

The main aspects regarding safety analysis, power production efficiency

and technical complexity were considered in selecting an appropriate ADS configuration. The point kinetic model with an external source assumes implicitly a uniformly distributed external source. In the ADS configuration, the external neutron source is however highly localized. The effect of this localization of the source on the multiplicity of the ADS and the external neutron source strength is analysed and assessed with respect to the reference system based on the point kinetic model. The actual location of the source within the core induces spatial changes in the flux distribution. Each of the above mentioned configurations exhibits its own particular characteristics in regards to the multiplicity factor and the power level on the core side and the strength and intensity of the beam on the accelerator side. Consequently, based on safety and operational considerations one can choose the preferable core configuration.

The 3-D core simulation calculated with DIXY2 code, was already discussed for simpler geometry. Yet, the former results were aimed to stress out the impact of the external source on the reactivity coefficients, whereas this section examines the way to optimize the ADS configuration. The optimization is based on calculations with the 3-D hexagonal option of the CITATION code. The cross section were calculated by KARBUS code package. The results are plotted separately for each effect in figures 11-13.

Fig. 11 shows the multiplicity deviation of the three options from the reference homogeneous criticality factor as a function of the system's subcriticality. The central source configuration exhibits a negative slope with increasing K_{eff}, whereas the three and six sources systems have a positive slope. This means that by insertion of a positive reactivity ramp the one source system will inherently reduce the positive ramp in comparison with the reference core. The three sources system has a very moderate slope and will practically behave like the reference system while the six sources system will "amplify" the reactivity ramp by reducing its previous negative subcriticality. An additional aspect seen in Fig. 11 is the core behavior after shutting off the sources. The central source shut down is always accompanied by a desired decrease in the criticality. The three source system has only a minor criticality increase when the sources are shut down. The six sources option leads to a large positive reactivity insertion following a shutdown of the sources. This could undermine the system stability.

Fig. 12 describes the dependency of the peak factor on the subcriticality for the three configurations. The peak factors shown are based on the ratio between the maximal power (based on a CITATION mesh design) and the average power distribution. The reference value for each system is its value at $K_{eff} = 1$ (which is equal to any source free subcriticality state). The advantage of six sources system is well demonstrated as it has the lowest peak factor (down to 1.63). The central source can reach a $3.6 - 4$ peak factor in the relevant K_{eff}

range which is far from an acceptable value. (At the most 2.5, before improving it by means of thermohydraulic methods). The minimum values for the three and six sources curves (Fig. 12) results from the peak factor position. At further lower subcriticalities the sources are governing the power shape and the peak factor is adjacent to the source (for example at the closest inner fuel element to the source, SA 22 in Fig. 10). At reduced subcriticality (K_{eff} approaching one) the peak factor is located at the center zone of the core. The minimum peak factor is reached when the center SA and the SA's adjacent to the sources have similar power levels. This flatting phenomenon of the power is plotted in Fig 14,15. Fig 14 shows the normalized power distribution for a source free case of the three sources configuration having a peak factor of 2.55 in the center of the core. Adjacent to the inner lead coolant cavity (for example SA 22), the power is 75% of the peak power. At the outer side of the cavity (sixth ring from the center in Fig. 10) the power decreases to only 25% of the center peak power. When the sources are activated a "plateau" of the same power level is spread between the inner sides of the power cavities through the core center (Fig. 15). In this case the fuel elements on the outer sides of the power cavities produces 40% of the center fuel elements. Thus the overall peak factor is reduced by almost 10% in comparison with the reference model. The three sources options has therefore an initial acceptable peak factor value which after thermal improvements can be decrease further to an operating level (below two).

In Fig 13. the operational aspect of the optimization are plotted. Besides the additional costs of designing three or six sources instead of one, due to the enhanced leakage rate of the multiple sources systems, the overall strength of the multiple sources is larger than the central source. For example, around 45% more current in the accelerator is needed for the three sources system if one wants to maintain the same power level of an equivalent central source configuration. For the six sources configuration where the leakage is considerably large, the additional strength is three times and more in comparison with the central source, depending on the source free core criticality. In particular, above $K_{eff} = 0.94$ the strength of each of the six sources must be higher than each of the sources in the three sources configurations. From an operational viewpoint, this rules out the specific six sources option investigated.

The characteristics of the three configurations leads at the moment to the conclusion, a three source system is favorable as its features are technical achievable. Yet other configurations could be better depending on improvements in the accelerator current, heat removal from the target and reduction techniques of the peak factor. Furthermore, this study was carried out with fresh fuel and other results could be expected for burned fuel during the core lifetime, or if the fuel will be mixed with transmutable fission products.

4.4 Procedure of feedback coefficients insertion into SAS4A input

The corollary of chapter 3 is that the use of perturbation theory is not available, for ADS. Therefore, the coefficients must be evaluated directly using exact calculation of the perturbed system reactivity and subtracting the unperturbed system reactivity from it. This is more complicated to do than the current linkage through AUDI3 code, and in addition consumes more computation time (even though the time could be reduced by special acceleration techniques). On the other hand, the coefficients will be obviously more accurate using exact calculations. The elaborated procedure evolves a script which arrange for each perturbation the correct cross-section set and then the CITATION code is used to evaluate the reactivity of the perturbed core. After each of the reactivity feedbacks needed in SAS4A was computed, a special routine will arrange the data in a suitable form for the input block data "POWINC" of SAS4A. The transfer of data from the cross-section data file to CITATION input has been already automized by a special KAPROS module (CTFILE). Thus, based on a SAS4A channel structure, the reactivity feedback of any perturbation in each of the fuel segments can be analyzed. Next, the whole data must be organized so it can be implemented in the SAS4A input file, in particular into the restart options. This latter step must be incorporated with a rigorous study of the ADS features, regarding the essential changes in the code due to the lead coolant.

5 Summary and Conclusions

The current study was aimed to adapt the SAS4A code for ADS simulation. It was shown that the code is capable of calculating the overall transient phenomena of an ADS. The ability of the code to handle the external source problem with relatively few modifications lies in the separation between the kinetic part (which is done by a point kinetic model) and the spatial contribution which is implemented implicitly within the feedback reactivity coefficients and the power distribution. Thus, the source appears as an additional term in the point kinetic equation and the solution technique is valid.

The SAS4A point kinetic model is justified for source free problems as the changes in the flux shape are considered to be small during most of the transients. For ADS simulation, one is forced to use the point kinetic model for transients simulation as this is (so far) the only time dependent inhomogeneous scheme which has a "close" solution. Yet, contrary to the homogeneous case the spatial flux distribution is more sensitive to local changes in the core and therefore a modified flux (power) distribution must be incorporated every several time intervals, during the transient simulation. This should be done by using the restart option of the SAS4A code to update the feedback reactivity coefficients and the power distribution (which includes implicitly the spatial flux shape). This method leads to an additional complexity namely the conservation of the same channel structure of the specific simulation during a restart.

A full 3-D spatial kinetic time dependent, inhomogeneous (external source) model has not yet been mathematically proven. Such a solution is essential for advanced developments concerning the ADS project. The complexity of this problem is the combination between a transient term and an inhomogeneous Helmholtz equation.

The generation of correct feedback reactivity coefficients for SAS4A input was the main goal of this study. For homogeneous (source free) cores they are easily calculated by means of first order perturbation theory. In such a way the coefficients are obtained rather quickly. However as was shown in the current work, for some void insertions, first order perturbation theory lack the needed accuracy even for homogeneous problems. When an external source is considered the flux shape is even more sensitive to disturbances during a transient. Therefore, the range of validity of first order perturbation theory is expected to be significantly smaller. Moreover, the formulation of perturbation theory is more complicated, as there is no unique definition for the adjoint flux (used as the weighting function). From the current and previous studies, it is not even sure if such a unique definition exists for inhomogeneous problems.

Consequently, one has to calculate the exact reactivity feedback coefficients (due to changes in temperature density etc.) separately for each of the SAS4A channel segments instead of using perturbation theory. This will enhance considerably the computational time compared to first order perturbation theory technique. Yet, for ADS calculation it is the only possible way to achieve accurate results. Furthermore, the computational time needed is estimated to be acceptable.

The diffusion codes available in FZK were found to be accurate for ADS flux simulation. Nevertheless, from the current study it was pointed out that the AUDI3 code, which links the diffusion calculations with the SAS4A input data, was not capable of handling source problems due to its numeric scheme that fails to evaluate the leakage term properly. The leakage term is needed to calculate the multiplicity factor which cannot be directly obtained (like in homogeneous cases) because there is no defined eigenvalue. To overcome the problem of AUDI3, the diffusion CITATION code was used. This code uses a different numeric scheme which allows for accurate leakage rates and thereafter, the multiplicity factor for an ADS can be calculated. The code option for a full 3-D hexagonal core was used to analyze different sources configurations. Three configuration were investigated for fresh fuel from which it was concluded, the three sources option is the most realistic. This result should be further analyzed to comply with the burn up conditions during the core lifetime. In addition, other optimized configurations could be thought of, depending on the amount and location of transmutable isotopes in the core, or improvements in the accelerator and target design.

In order to prepare the various reactivity coefficients needed for SAS4A input file, an automatic procedure was written which transfers the cross-section sets from the KARBUS routine package to the CITATION input file. A script to calculate all the perturbations successively exists too. An additional work is needed to form a mechanism for the automatic transfer of data from CITATION to SAS4A input data file in the correct form.

In the meantime an extensive study was carried out to modify the leakage term and it is possible to determine accurately the multiplicity factor also with D3D/D3E code. This enables the usage of the verified and well established transferring routines from D3D/AUDI3 to SAS4A. Further improvement is the direct coupling of SAS4A with CITATION code. Such an approach is complicated due to the channel structure of the SAS4A code, but can be developed [23].

6 References

1. "The SAS4A LMFBR Accident Analysis Code System", ANL/RAS 83-38 revision 2, February 1988.

2. J. J. Kaganove, "Numerical Solution of the One-Group Space-Independent Reactor Kinetics Equations for Neutron Density Given the Excess Reactivity", ANL-6132, Argonne National Laboratory 1960.

3. E. L. Fuller, "The Point Kinetics Algorithm for FX2", ANL-7910, Argonne National Laboratory, pp 503-508, 1972.

4. C. Rubbia et all, "Conceptual Design of a Fast Neutron Operated High Power Energy Amplifier" CERN/AT/95-44(ET)

5. W. Mascheck , B. Merck , FZK, private communication , 1998.

6. Broeders C.- "Entwicklungsarbeiten für die neutronenphysikalische Auslegung von Fortschrittlichen Druckwasserreaktoren (FDWR) mit Kompakten Dreiecksgittern in hexagonalen Brennelementen", KFK 5072, August 1992.

7. Stehle B. - D3D and D3E Zweige eines FORTRAN-Programms zur loesung der stationären dreidimensionalen Multigruppenneutronen in diffusiongleichungen in Rechteck-, Zylinder- und Dreieckgeometrie", KFK 4764 , April 1991.

8. Broeders C. , Broeders I. - "Neutronenphysikalische Analysen von Beschleunigergetriebenen unterkritischen Anordnungen", Nachrichten-FZK , No. 29, pp411-420, April 1997.

9. Ravetto, P. Pazsit I. "Theoretical basics of reactivity control for ADS"- Workshop on P. and T. Strategy studies and transmutation experiments, Karlsruhe ,17 -19 June , 1998.

10. STACEY W. M. - Space -Time Nuclear Reactor Kinetics , Nuclear Science and Technology 5, Academic press New-York 1969.

11. Askew J. R. et all. "A General Description of the Lattice Code WIMS", Journal Of British Nuclear Energy Society , 5, 564, 1966.

12. Ott K. and Menely D, "Accuracy of the Quasistatic Treatment of Spatial Reactor Kinetics, Nucl. Sci. Eng. 36,402, 1969.

13. Ott K. "Introductory Nuclear Reactor Dynamics", American Nuclear Society, ILL. U.S.A 1985.

14. Höbel W. , Ott. M. "Kurzbeschreibung und Benutzeranleitung der KAPROS- Prozedur DIXY2" INR-1287, FZK November 1983.

15. Weinberg A. and Wigner E. "The Physical Theory of Neutron Chain Reactors", University of Chicago Press, 1958.

16. Duderstadt J. and Hamilton L. "Nuclear Reactor Analysis", John Wiley and sons Inc. 1976.

17. Salvatores M. , Slessarev I. and Tchistiakov A., "The Transmutation of Long-Lived Fission Products by Neutron Irradiation", Nuc. Sci. Eng. 130, pp. 309-319, 1998.

18. Bell G. & Glasstone S. "Nuclear Reactor Theory", Van Nostrand Reinhold Company, 1970.

19. Willerding G. , "AUDI3 ein Programm fuer Stoerungs Rechnung 1. Ordnung", INR-1241 November 82.

20. Fowler T. B., Vondy D. R., Cunningham, "Nuclear Reactor Core Analysis Code: CITATION", ORNL-TM2496, Rev. 2 , 1971.

21. Broeders C. -"Distributed targets" , Workshop on P & T Strategy Studies and Transmutation Experiments, Karlsruhe 1998.

22. Knebel J. et all, "Untersuchungen zu beschleunigergetriebenen, unterkritischen Anlagenanordnungen", FZKA 6300, 1999.

23. Niwa, H., Kanazawa S. and Kurihara K. "Coupling with a Space-Time Kinetics Model", 11^{th} SAS4A Specialist Meeting, Karlsruhe, June 16-18, 1999.

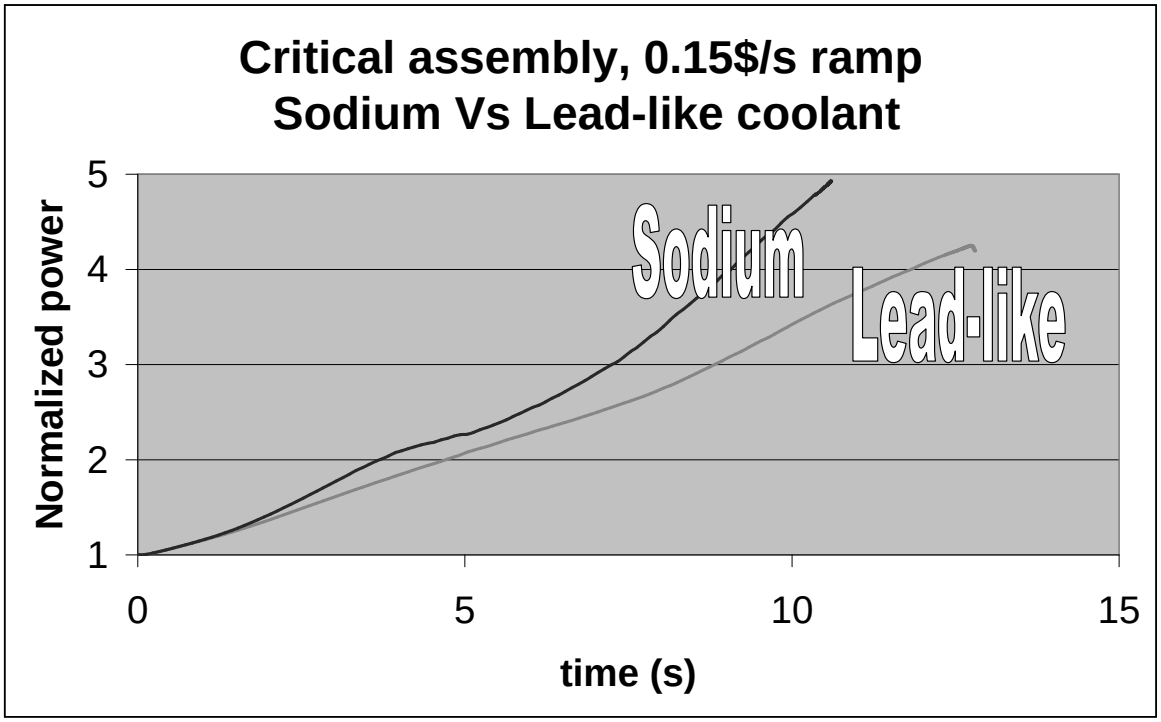

Figure 1: Comparison between sodium and lead-like coolant during a $0.15\$/s$ reactivity ramp starting at 0.1s. An initial critical core is considered.

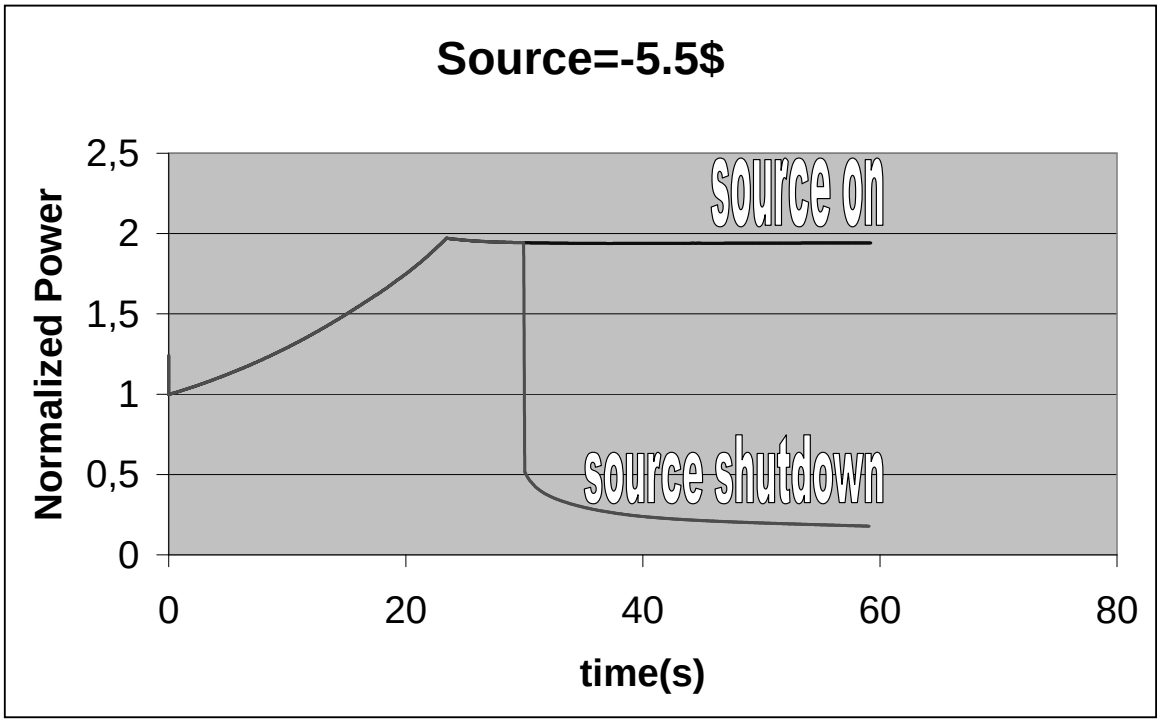

Figure 2: Power excursion during $0.15\$/s$ reactivity ramp starting at 0.1s. An initial subcritical core ($K_{eff} = 0.98$) with an external source (maintaining the same power level as in Fig.1).

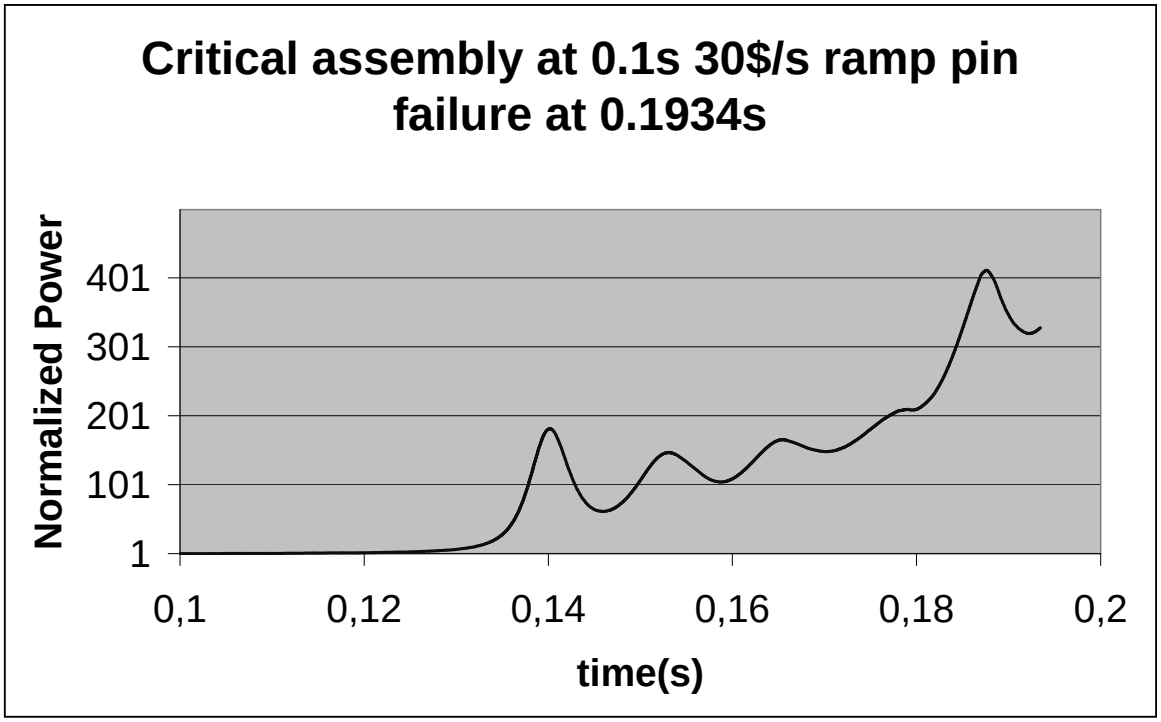

Figure 3: Power excursion during a $30\$/s$ reactivity ramp starting at 0.1s. An initial critical core is considered.

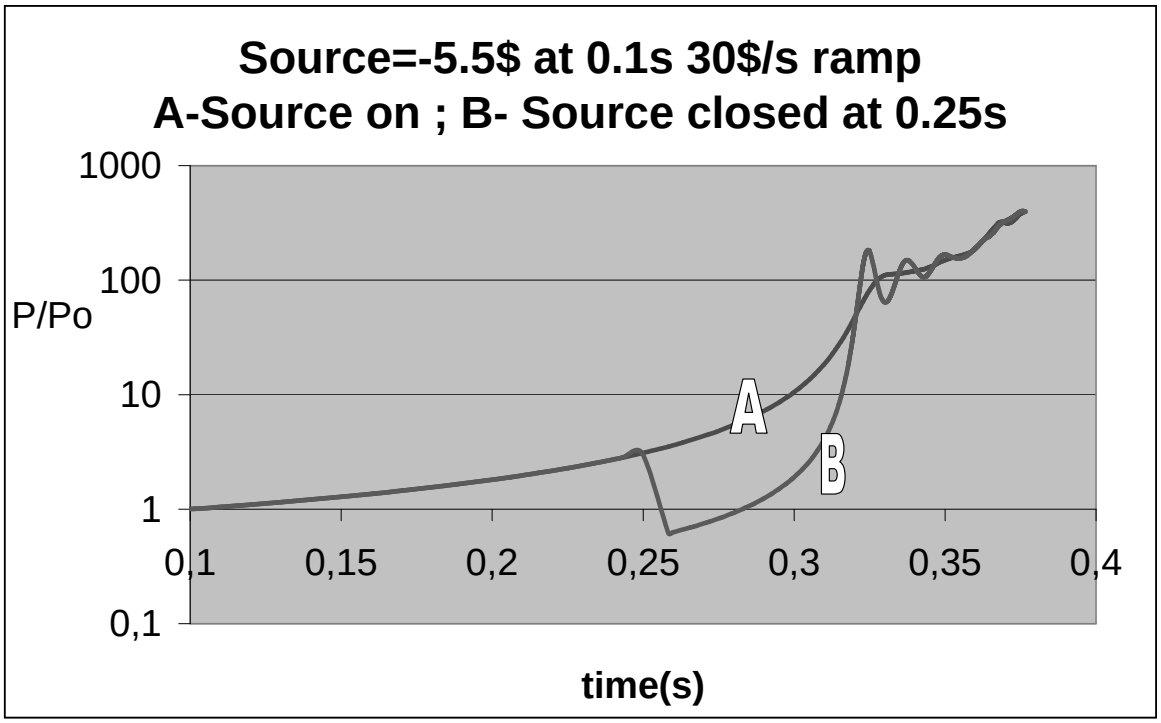

Figure 4: Power excursion during $30\$/s$ reactivity ramp starting at 0.1s. An initial subcritical core ($K_{eff} = 0.98$) with an external source (maintaining the same power level as in Fig.3).

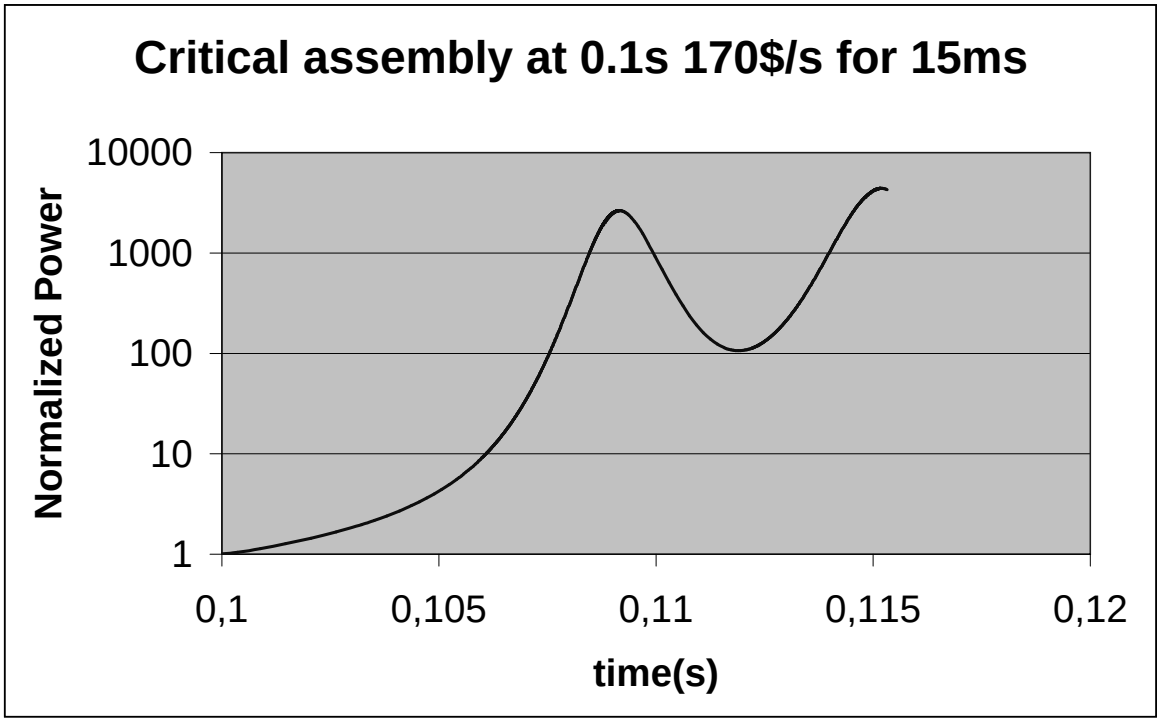

Figure 5: Power excursion during a 170$/s$ reactivity ramp for 15ms. starting at 0.1s. An initial critical core is considered.

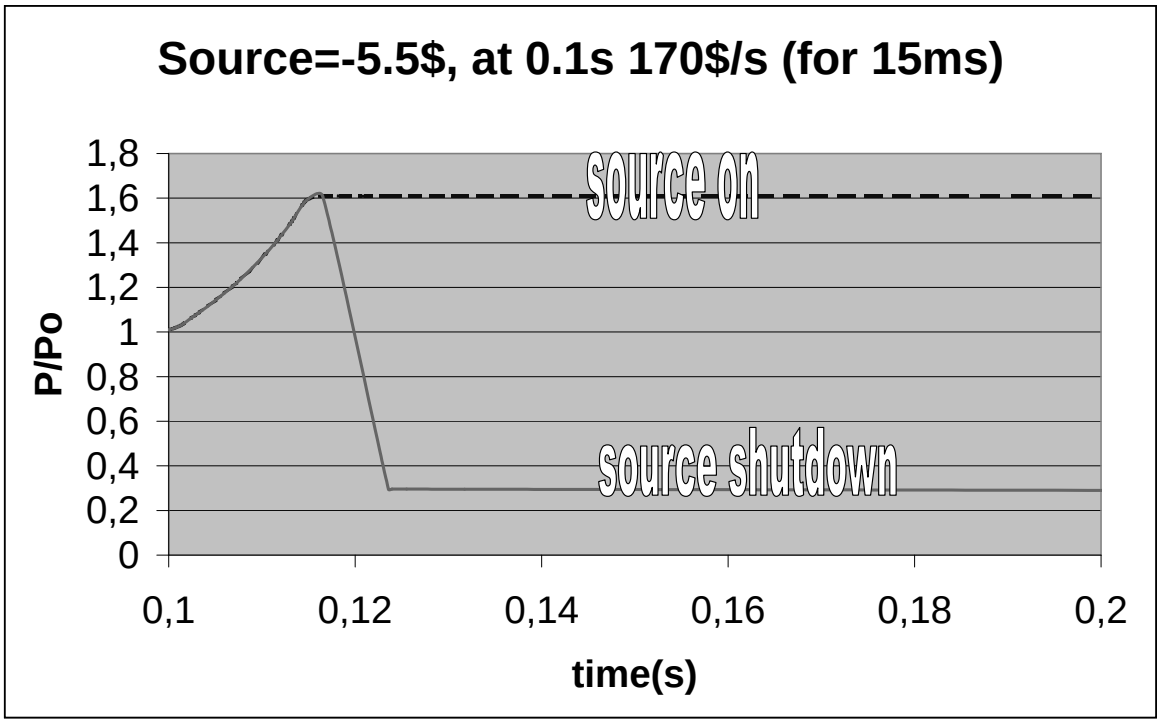

Figure 6: Power excursion during 170$/s$ reactivity ramp for 15ms starting at 0.1s. An initial subcritical core ($K_{eff} = 0.98$) with an external source (maintaining the same power level as in Fig.5).

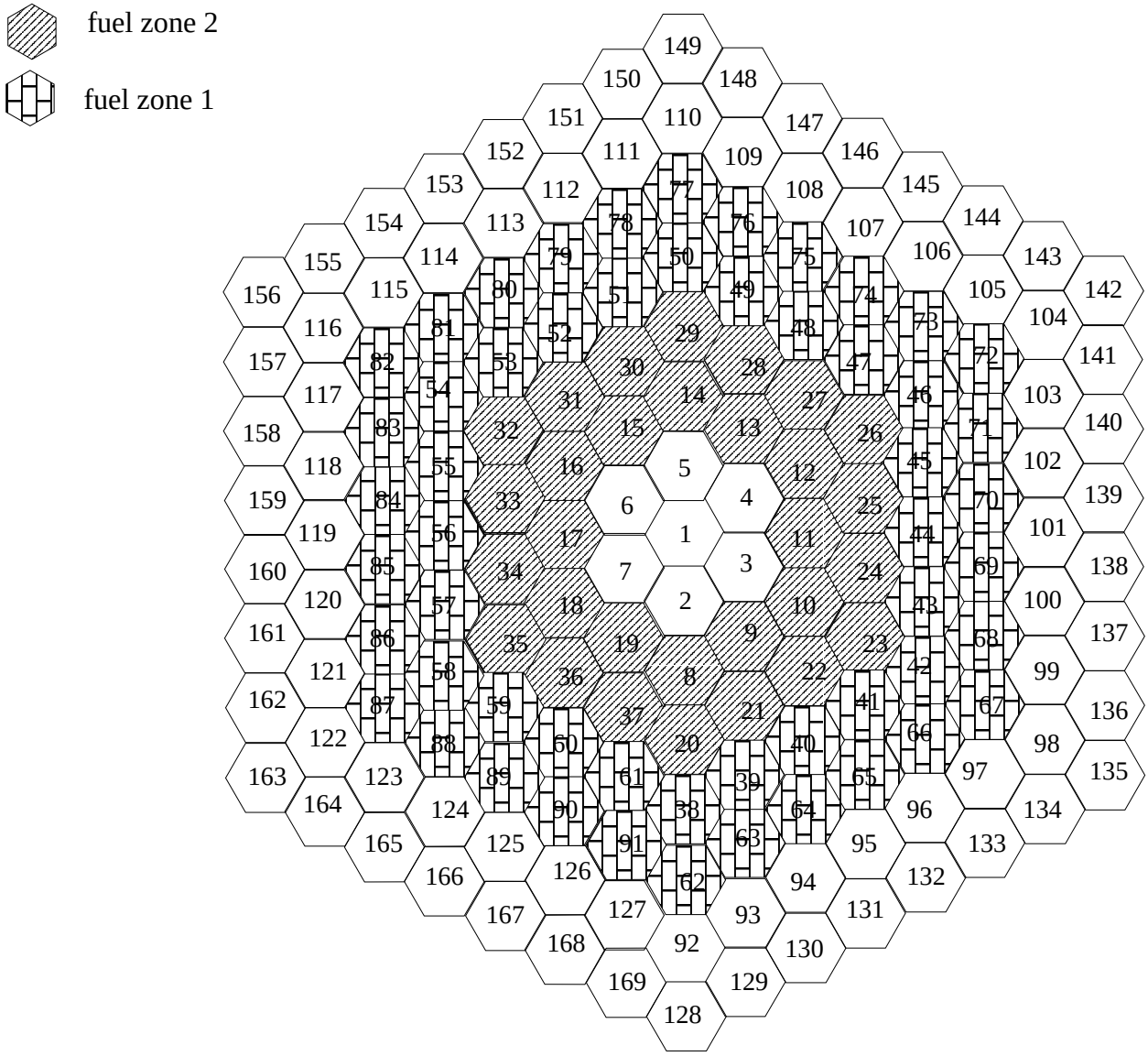

Figure 7: Hexagonal mid plane, central source core configuration loaded with uranium fuel, for 3-D diffusion calculation

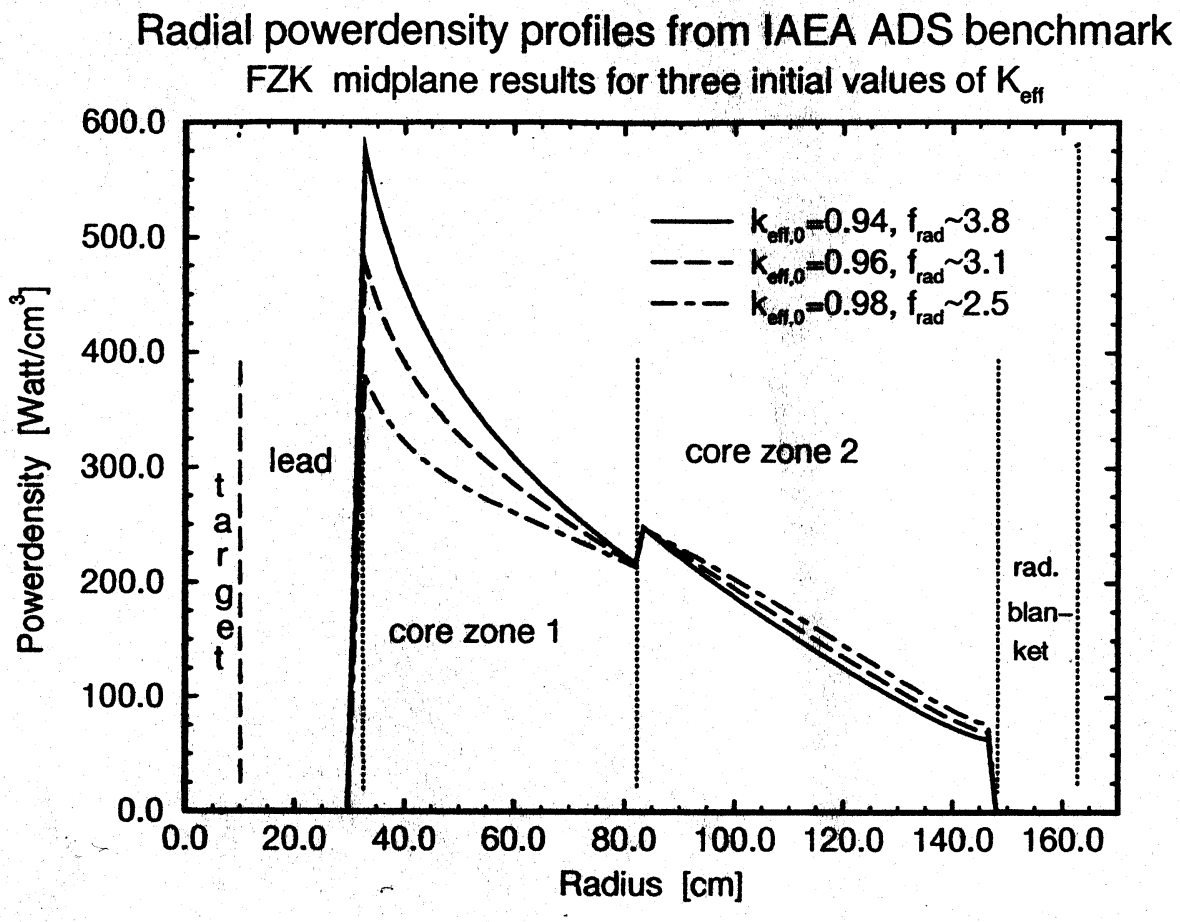

Figure 8: Radial power density profiles in an ADS with different criticality

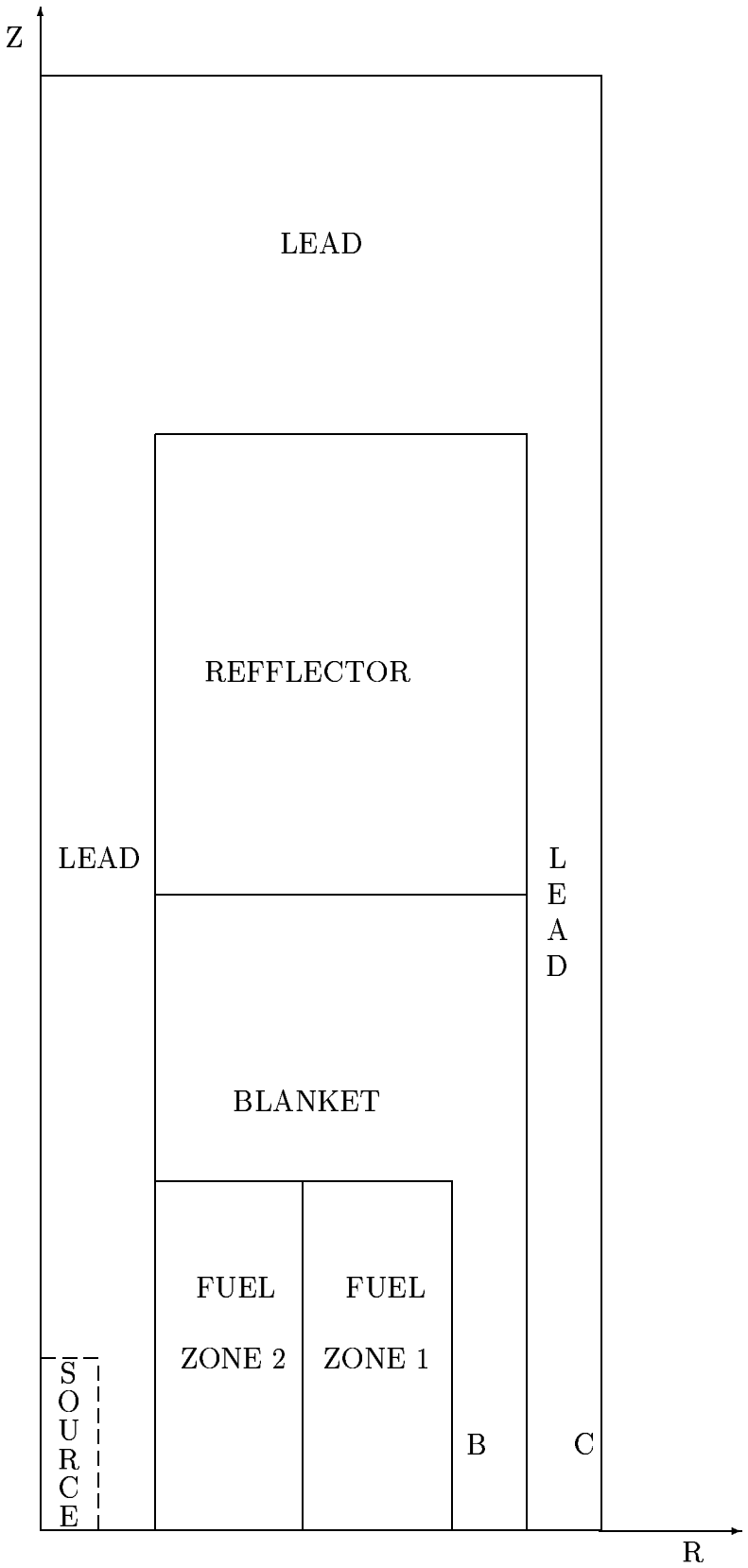

Figure 9: R-Z Core configuration for the reactivity feedback and multiplicity tests

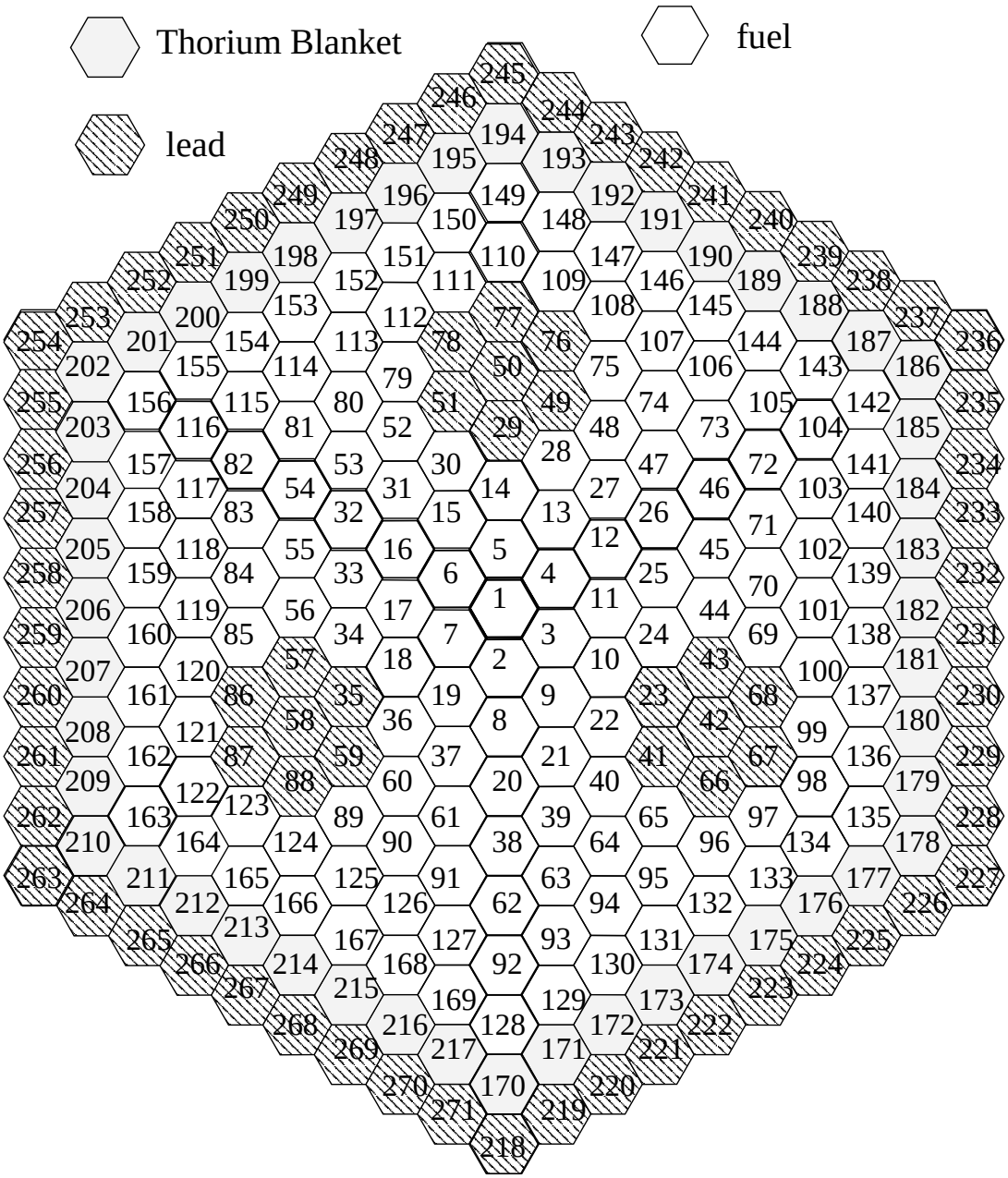

Figure 10: Hexagonal mid plane, 3 source core configurations loaded with thorium fuel, for 3-D diffusion calculation

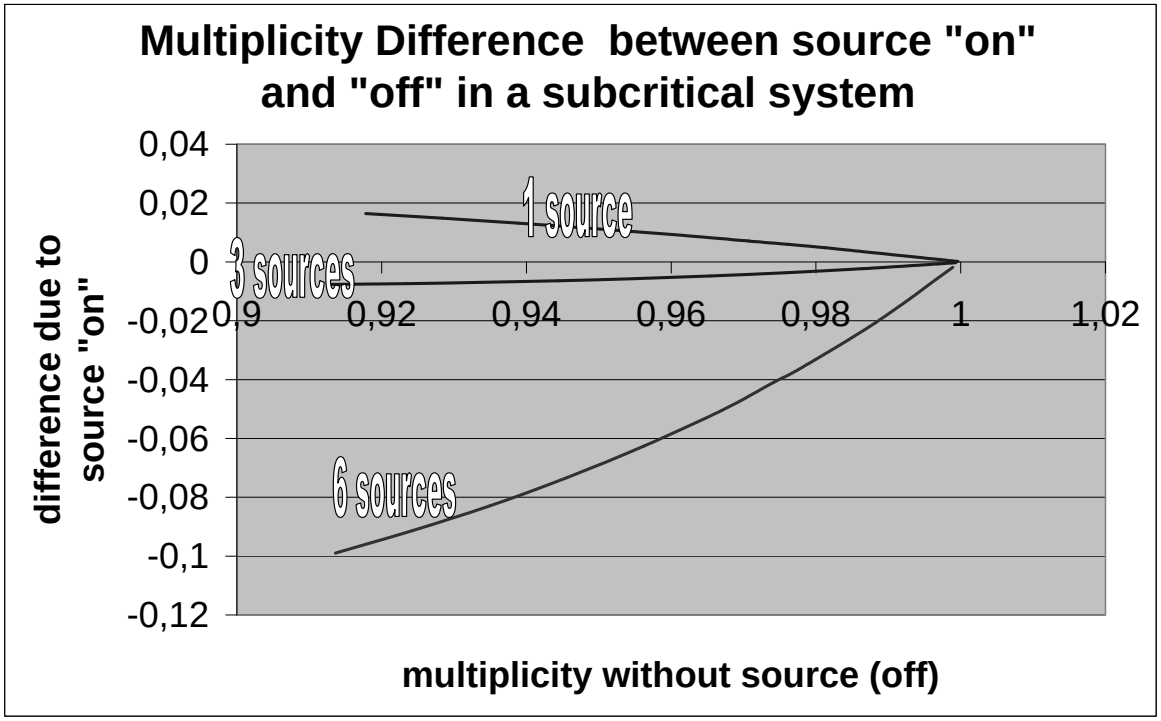

Figure 11: Change in multiplicity due to source(s) activation for 3 configurations. 1 central source, 3 sources (Fig. 10), 6 sources located in places 92,98,104,110,116, 122 (in Fig. 10)

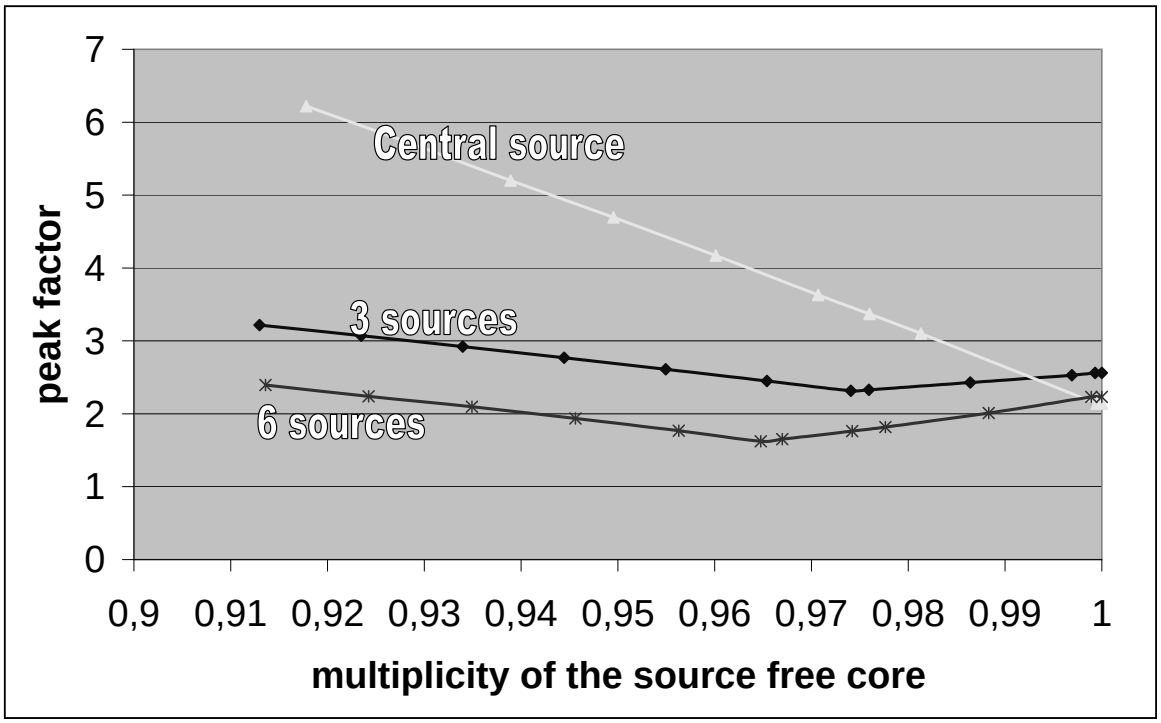

Figure 12: Peak factor for 3 configurations. Central source, 3 sources (Fig. 10), 6 sources located in places 92,98,104,110,116, 122 (in Fig. 10) (the value at 1.0 is the source free peak factor value for each configuration

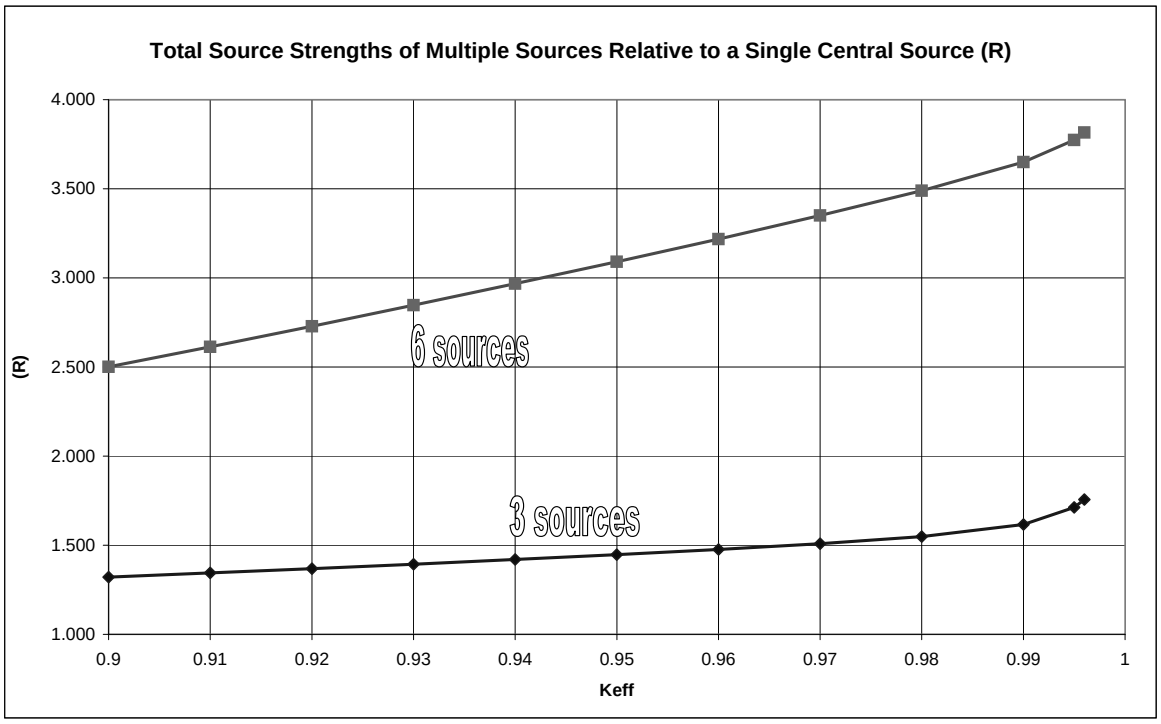

Figure 13: Total source strengths of multiple sources relative to a single source. 3 sources configuration (Fig 10) , for 6 sources the locations are in places: 92,98,104,110,116, 122 (in Fig. 10) K_{eff} refers to the source free core for each configuration

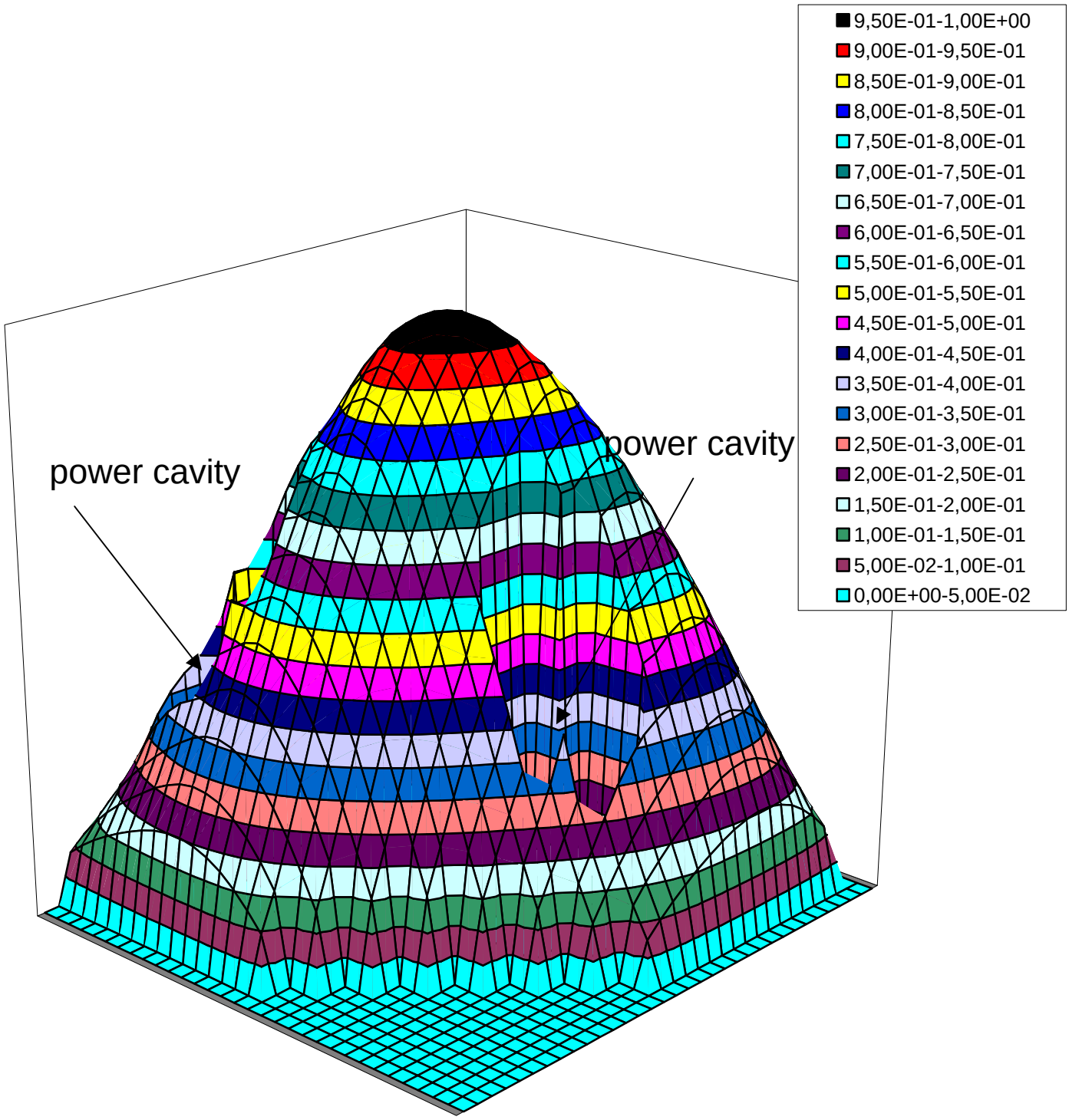

Figure 14: Normalized power distribution at mid plane for 3 sources configuration (sources "off"), peak factor 2.55

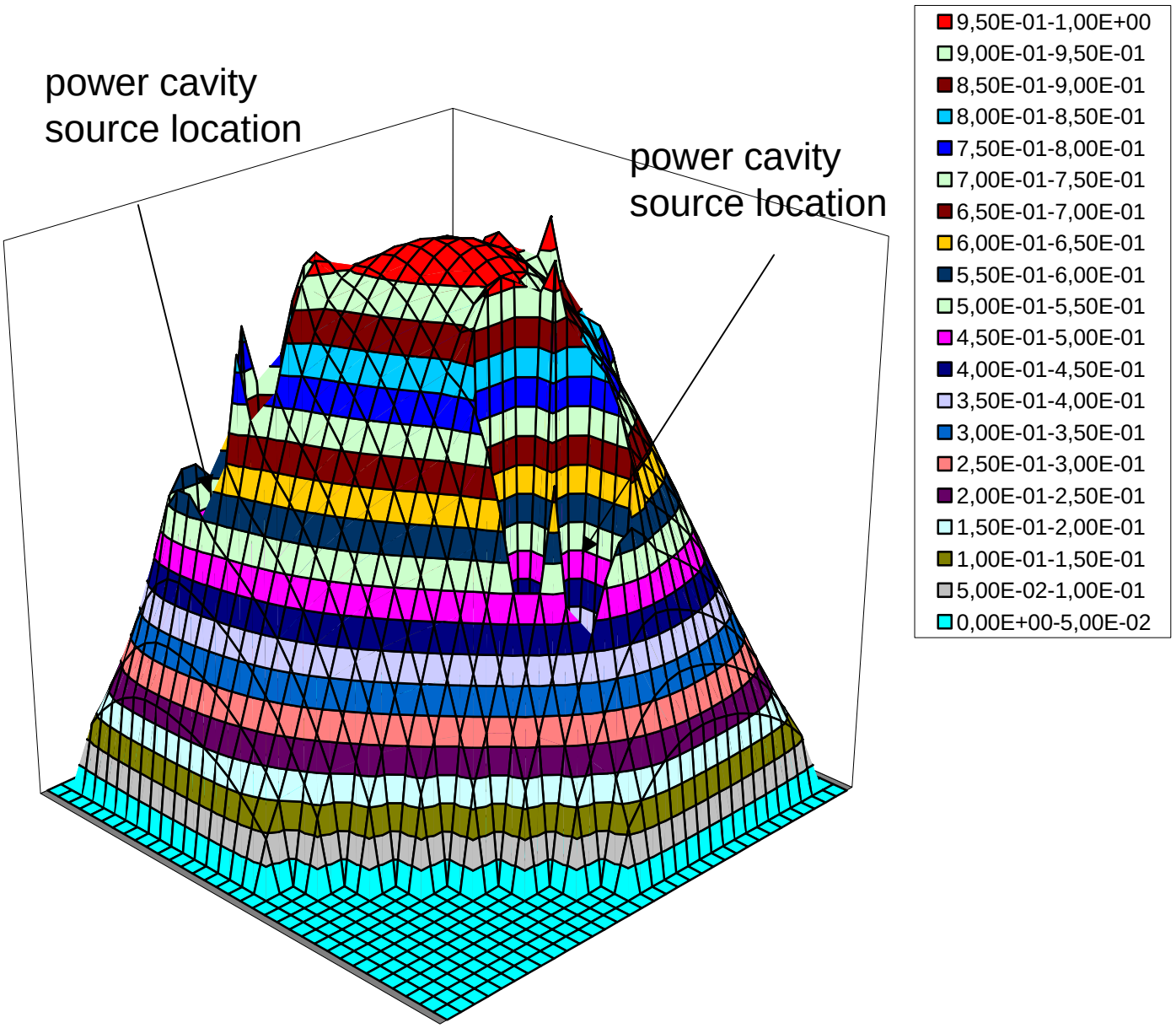

Figure 15: Normalized power distribution at mid plane for 3 sources configuration (sources "on"), peak factor 2.31